Journal of Structural Geology 60 (2014) 13–29

Contents lists available at ScienceDirect

Journal of Structural Geology

journal homepage: www.elsevier.com/locate/jsg

Inversion of pre-orogenic extensional basins in the external Western Alps: Structure, microstructures and restoration

Alexandre Boutoux [a,b,*], Nicolas Bellahsen [a,b], Olivier Lacombe [a,b], Anne Verlaguet [a,b], Frédéric Mouthereau [a,b]

[a] UPMC Univ. Paris 06, UMR 7193, ISTeP, F-75005 Paris, France
[b] CNRS, UMR 7193, ISTeP, F-75005 Paris, France

ARTICLE INFO

Article history:
Received 31 May 2013
Received in revised form
7 December 2013
Accepted 19 December 2013
Available online 31 December 2013

Keywords:
Shear zones
Dysharmonic folding
Balanced cross-section
Finite strain ellipsoids
Western Alps

ABSTRACT

During collision, continental margins are shortened along with the inversion inherited syn-rift basins. In this contribution, we explore the internal deformation of pre-orogenic basins during their inversion in the external Western Alps. New structural and microstructural data allow us to provide a new kinematic scenario for the shortening of two inherited basins in the Oisans External Crystalline Massif. Two cleavages and three vein sets are documented by field observations in the sedimentary cover metamorphosed in the greenschist facies. Their spatial and temporal development is strongly dependent on the structural style that is controlled by the initial basin geometry. In the basement, shear zones accommodate the shortening while the cover is disharmonically folded. We present a new approach for the restoration of cross-sections where ductile deformation prevailed, thus for which classical methods do not apply. Both length conservation for basement top and area conservation for the sedimentary cover, as well as fixed hinge kinematics for the cover folds, are assumed. Such restoration is discussed in the light of cover strain ellipsoid quantification based on field data analysis. We apply this approach to the Morcles nappe and propose a new restored geometry, which is further compared to the Oisans section.

1. Introduction

Continental collision occurs when proximal continental margins get shortened during convergence. During such events, the inherited syn-rift basins are inverted, with normal fault reactivation (Letouzey et al., 1990; Roure and Colletta, 1996; Lacombe and Mouthereau, 2002; Mouthereau and Lacombe, 2006) or not (Butler, 1989; Tavarnelli, 1999; Scisciani et al., 2002; Buiter and Pfiffner, 2003; Panien et al., 2005; Butler et al., 2006). In particular, tectonic burial has been suggested to inhibit normal fault reactivation (Bellahsen et al., 2012): indeed, the P–T conditions that prevail during collisional shortening associated to the intrinsic weakness of syn-rift marly sedimentary rocks may significantly weaken the crust, down to the strength of the inherited faults. In such case, the inverted inherited basins exhibit strong internal ductile deformation (e.g., cleavage) that affects the metasedimentary cover. The tectonic burial, as well as the inherited structure of the lithosphere (Watts et al., 1995; Mouthereau et al., 2003), also control the structural style during shortening: a rather hot lithosphere most likely deforms with a thick-skinned structural style.

One problem in such setting is the balancing of cross-sections because ductile deformation precludes any use of classical methods of restoration. The methodology of balanced cross-section was established since Chamberlin (1910) and Dahlstrom (1969) essentially in the external parts of orogens by using length or area conservation, as deformations are mainly brittle. In this case, balanced cross-sections provide key insights on the structural style and on the amount of shortening. Recently, new approaches have been proposed to balance cross-sections, not based into length conservation but only into area conservation in order to take into account the internal deformation of the layers (Epard and Groshong, 1993; Groshong and Epard, 1994; Bellahsen et al., 2012; Moretti and Callot, 2012; Butler, 2013). These recent approaches allow balancing ductile deformation but do not take into account the analysis of finite strain from field data.

In internal domains of many collisional orogens, key data on both the precise amount and the kinematics of collisional

* Corresponding author. Université Pierre et Marie Curie, ISTeP, UMR 7193 UPMC-CNRS, Case 129 T46-00, 2eme étage, 4 place Jussieu, 75252 Paris Cedex 05, France. Tel.: + 33 1 44 27 71 81; fax: + 33 1 44 27 50 85.
E-mail address: alexandre.boutoux@upmc.fr (A. Boutoux).

0191-8141/$ – see front matter © 2014 Elsevier Ltd. All rights reserved.
http://dx.doi.org/10.1016/j.jsg.2013.12.014

shortening are still missing. This is mainly due to the lack of clear strain/kinematical markers as collisional shortening is superimposed onto subduction-related deformation and metamorphism and/or to significant ductile deformation. In the external Western Alps (Fig. 1), during the continental collision that started during early Oligocene times, the proximal European continental margin has been tectonically buried below the internal (Penninic) units down to the brittle–ductile transition (e.g. Crouzet et al., 2001; Simon-Labric et al., 2009; for the Oisans massifs: Fig. 1). In such a setting, inherited normal faults were not reactivated and the structural style is thick-skinned in the pre-orogenic extensional basins and locally thin-skinned where the crust was not previously significantly thinned (Bellahsen et al., 2012). Thus, if the shortening of the alpine external zones is now well-constrained (Guellec et al., 1990; Mugnier et al., 1990; Ford, 1996; Burkhard and Sommaruga, 1998; Deville and Sassi, 2006; Bellahsen et al., 2012), second-order variations in structure and kinematics require refinements.

This paper aims at providing new structural and microstructural data to better constrain the kinematics of inversion of pre-orogenic syn-rift basins in the Oisans External Crystalline Massif (ECM, Fig. 1). We especially show that the spatial and temporal development of cleavages and vein sets depends on the structural style that is itself controlled by the initial basin geometry. We also propose a new approach to balance cross-sections in such settings where significant ductile deformation precludes the use of the classical length conservation hypothesis. In this approach, we then assume for the North Oisans basins a constant length for the basement top and a constant area for the sedimentary cover. The sedimentary layer length variations predicted by the restoration are validated *a posteriori* with field-derived data on finite strain. This technique is also applied to the Morcles nappe in the Aiguilles Rouges-Mont Blanc ECM (Fig. 1). The comparison between Oisans and Aiguilles Rouges-Mont Blanc ECM further provides new insights into the variations of the accommodation of collisional shortening along the strike of the Alpine arc.

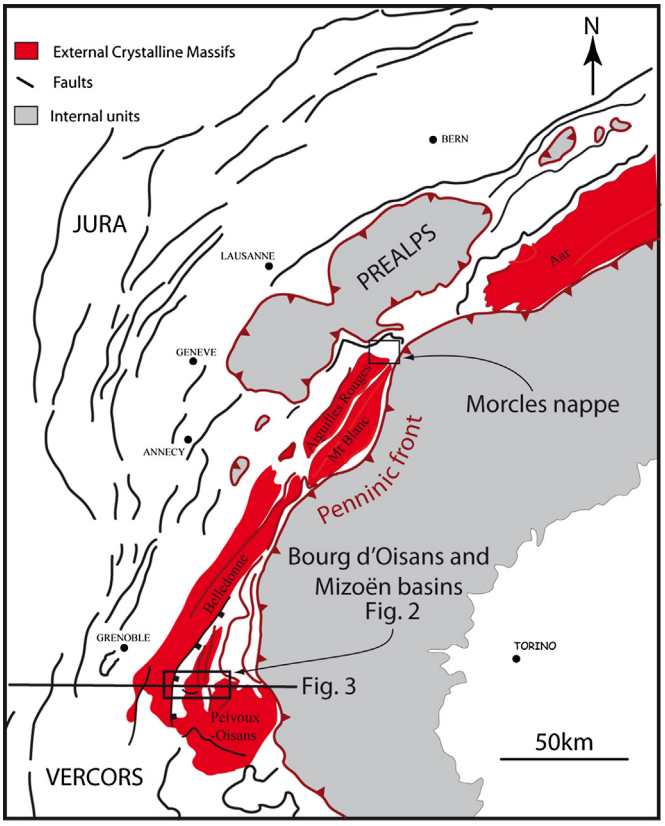

Fig. 1. Location of the studied area in western Alps. The frame in the northwestern Oisans massif represents the map in Fig. 2. The straight line indicates the cross-section of Fig. 3.

2. Geological setting

The Alps are the result of the closure of the Ligurian part of the Tethyan ocean (Lemoine et al., 1986). The ECM in Western Alps (Fig. 1) represent the inverted proximal European continental margin of the Ligurian ocean, where rifting occurred during Liassic and Dogger times, as attested by several N–S to NE–SW half-grabens. These basins are bounded by normal faults that controlled the deposition of marly syn-rift Liassic and Dogger series (Barféty et al., 1979; Lemoine et al., 1981, 1986; Lemoine and Tricart, 1986; De Graciansky et al., 1989). In southeastern Oisans, from the end of Dogger to Cretaceous, a thick post-rift sedimentary cover was deposited, but most of it has subsequently been eroded (Fig. 1).

The subduction of the Ligurian ocean began during Cretaceous and ended during Eocene times, with the continental subduction of the distal parts of the European margin (Butler, 1986; Chopin, 1987). Then, the collision started at about 30–35 Ma with shortening of the proximal margin and final exhumation of the internal units (e.g., Rolland et al., 2008; Simon-Labric et al., 2009; Van Der Beek et al., 2010; Sanchez et al., 2011). During this Oligo-Miocene phase, the external units (the so-called Dauphinois units) were tectonically buried below the internal units with the activation of the Penninic Frontal Thrust (PFT) and coevally underwent metamorphism under greenschist facies P–T conditions. The ECM experienced peak temperatures of 280–350 °C (Crouzet et al., 2001; Simon-Labric et al., 2009), which suggests that they reached about 10 km depth assuming a 30 °C "normal geotherm". During the Alpine shortening, the structural style was thick-skinned and no major decollement occurred between the cover and the basement, most likely because of the low crustal strength under collisional greenschist facies P–T conditions. Few hundred meter-thick shear zones deformed the basement while the cover was disharmonically folded over these shear zones (Bellahsen et al., 2012).

At the latitude of our study area (Figs. 1 and 2), two main inherited Jurassic half-grabens can still be recognized. The Bourg d'Oisans basin (Figs. 2 and 3) is limited to the West by the Ornon normal fault, which has a Jurassic throw of about 3000 m (Tricart and Lemoine, 1986; Lemoine et al., 1989) and was not significantly reactivated during the Alpine shortening (Fig. 3; Tricart and Lemoine, 1986). The pre-rift series consist of thin Triassic sandstones and dolomites and lower Liassic limestones and represent the cover that remained attached to the basement. The geometry of these Triassic (and lower Liassic) layers will be used in this study as a reliable proxy for the basement top geometry. The syn-rift deposits are Liassic to Dogger in age and are essentially marls and marly limestones with thicknesses varying from a few tens of meters on the crest of tilted blocks (Croix de Cassini and Emparis plateau, Fig. 2) to 2–3 km near the border normal faults (La Paute and Mizoën, Fig. 2). The post-rift sedimentary rocks have been significantly eroded and can only be observed at one locality (Le Grand Renaud, Fig. 2): they consist of a few hundred meters of upper Jurassic and Cretaceous limestones and marls. The Mizoën basin (Figs. 2 and 3) is limited to the West by the Mizoën normal fault, whose Jurassic throw is lower than that of the Ornon fault (about 2.5 km). The pre-rift series are similar to those observed in the Bourg d'Oisans basin; the post-rift sedimentary rocks do not crop out in this basin. Syn-rift subsidence and normal fault activity started a few million years later in the Mizoën basin than in the Bourg d'Oisans one (Barbier et al., 1973).

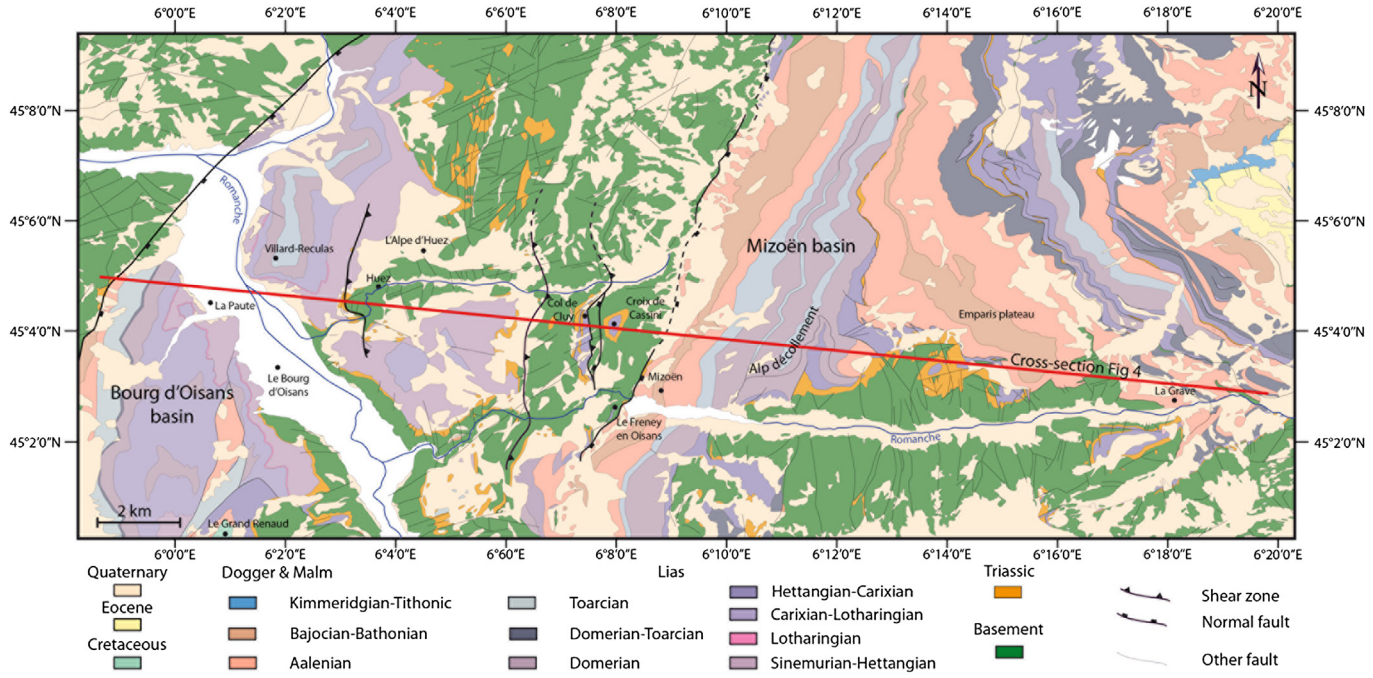

Fig. 2. Geological map of the Bourg d'Oisans and Mizoën basins, modified after Barféty et al. (1972) and Barbier et al. (1973). The Ornon and Mizoën normal faults and the basement shear zones are highlighted. The red line indicates the cross-section of Fig. 3. [For interpretation of color referred in this figure legend, the reader is referred to web version of the article.]

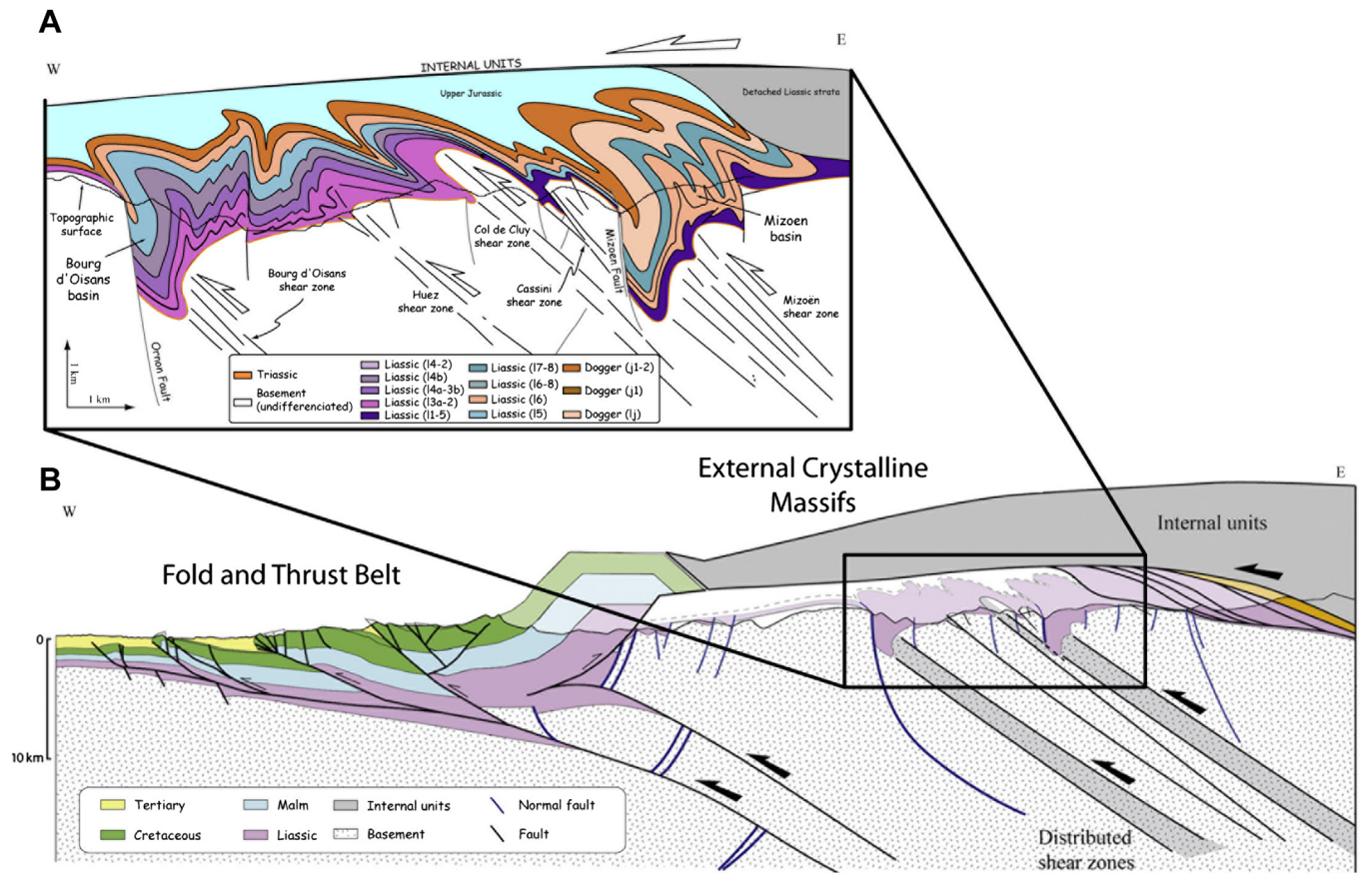

Fig. 3. Cross-sections after Bellahsen et al. (2012). A: Cross-section of the Mizoën and the Bourg d'Oisans basins. B: Bed-length and constant area balanced cross-section of the external zone. See location on Fig. 1.

3. Balanced cross-section and restoration

3.1. Restoration method

In the external Western Alps, the fold-and-thrust belts can reliably be balanced using constant length assumption for the Mesozoic layers (e.g., Philippe et al., 1998; Deville and Chauvière, 2000; Affolter et al., 2008). Dahlstrom (1969) established the conservation of the layer length and area during brittle deformation. In the innermost part of the Alpine external zone (i.e., in the ECM), deformation is partly ductile and metasedimentary layers are strongly internally deformed (Gratier and Vialon, 1980; Beach, 1982). Bellahsen et al. (2012) provided a balanced cross-section of the external zone at the latitude of northern Oisans (Figs. 1 and 3) by restoring the initial geometry of the Triassic layer, which is widely cropping out and is the best proxy for the basement top geometry. The Jurassic layers were restored under the assumption that their total surface is conserved during shortening. Indeed, Moretti and Callot (2012) underlined the occurrence of length variation of internally deformed strata due to pressure solution during shortening. Here, in order to balance the cross-section (Fig. 4), we propose a new approach based on these recent contributions.

During shortening and burial of marly layers, internal deformation mainly occurred through pressure-solution and mass diffusion at the cm- to dm-scale (Gratier et al., 1973; Henry et al., 1996; Oliver, 1996). Furthermore, we assume that there was no material displacement outside areas bounded by both stratigraphic interfaces and fold axial surfaces, as folds develop with fixed hinges. Finally, as only few veins are parallel to the cross-section (see further down and in Gratier et al., 1973; Gratier and Vialon, 1980), there was probably no flow perpendicular to the cross-section. As the section furthermore strikes parallel to the Alpine stretching lineations (i.e., E–W, see further down), area conservation during Alpine shortening appears to be a robust assumption. Practically, the Triassic layer length is first restored assuming a pre-collision geometry given by the Jurassic normal fault throw (about 3000 m) and a low dip for Triassic layers (5.5°), as another major assumption for restoration purposes is that no significant reactivation of the inherited Jurassic normal faults occurred during collision. Then, both the whole Jurassic layers and each of their cells defined by stratigraphic limits and fold axial surfaces are restored considering constant area (Fig. 5).

The lower Triassic layers are then used as proxies to characterize the basement top shape and to quantify basement shortening. These layers show some internal deformation: field observations indicate that they were stretched (as attested by bed perpendicular veins) and sheared (as witnessed by sigmoidal cleavage). Considering constant width shear zones, the Triassic layer length, when deformed within a basement shear zone, suffered length variations: a decrease followed by an increase (Bellahsen et al., 2012). In the Bourg d'Oisans basin, considering the geometry of the observed shear zones, the cumulated length variation is a lengthening of about 500 m (with an initial length of 14.5 km). Thus, the error is less than 4% and has been neglected in the restoration.

The two basins were restored to their geometry before any tectonic burial and after the end of post-rift sediment deposition, which implies that the restoration does not need to take into account the volume variation due to porosity loss during diagenesis.

3.2. Basement shear zones

In the Bourg d'Oisans basin, Alpine shortening in the basement has been accommodated by four main shear zones: the Bourg d'Oisans, La Garde, Col de Cluy, and Cassini shear zones (Fig. 4). The Bourg d'Oisans shear zone is only inferred as no basement rocks crop out in the Bourg d'Oisans area. However, it is likely that such a basement shear zone exists as lower Liassic rocks can be observed 2 km East of the Ornon normal fault (Fig. 2) indicating basement uplift. The Cassini shear zone is only poorly exposed, although its displacement is well constrained by the geological map (Fig. 2; Barféty et al., 1972). The two other shear zones can be observed and documented in the field (Fig. 4). These shear zones cut across and deform the Variscan foliation and dip at shallower angle (i.e., 30–50° to the East, compared to the 70° East-dipping Variscan foliation). The restoration of the Triassic cover–basement interface provides shortening values of 4.3 km (29%) for the Bourg d'Oisans basin.

In the Mizoën basin, basement deformation cannot be easily documented, due to the lack of exposure. However, its shortening can be estimated by the restoration of the Triassic cover–basement interface, which provides shortening values of 2.7 km (24%) for the Mizoën basin.

3.3. Cover folds

Five main cover folds, located above the basement shear zones can be mapped in the Bourg d'Oisans basin (Figs. 2 and 4). They are disharmonic folds and/or folds slightly detached from the basement (Fig. 4). Whatever the type, folding is here always associated with internal layer deformation. The upward extension of these folds is controlled by the restoration hypothesis of constant area. The area drawn on the cross-section must fit the restored syn-rift basin geometry based on the Triassic layer length and the dip of the normal fault throw. The geometry of all the folds and their East-dipping axial surface are consistent with a top-to-the-West shearing of the cover.

The location of the Liassic depocenters close to their associated normal faults and the strong link between cover folds and basement shear zones imply that no significant décollement occurred between the cover and the basement. However, where the cover folds are tight and their axial surfaces rather steep (above the Bourg d'Oisans shear zone, Fig. 4A), short décollements occur within the lower Liassic layers (Sinemurian–Hettangian). The layers of the Bourg d'Oisans metasedimentary cover show internal deformation (thinning of the fold limbs and thickening of fold hinges, Fig. 3), which makes shortening computations very complicated. However, because there is no large décollement of the meta sedimentary cover, cover shortening has to be similar to basement shortening.

Deformations of the Mizoën basin show slight differences with deformations of the Bourg d'Oisans basin, although the cover is also strongly folded and displays East-dipping fold axial surfaces. The main difference is the activation, in the Mizoën basin, of a décollement (the Alp décollement, Figs. 2 and 4A) restricted to the eastern part of the basin and localized within the Sinemurian layer. Under this décollement, two small-scale folds are associated with an East-verging shear zone within the cover (Fig. 4A). At a large scale, the eastern part of the basin consists of the Emparis Plateau (Fig. 4A), where the strata are thin and overthrusted by a meta-sedimentary nappe, usually mapped as Ultra-Dauphinois (Figs. 2 and 4; Ceriani et al., 2001) that probably roots further East. Because of uncertainties in this nappe rooting, the Mizoën basin is only balanced considering Triassic length preservation, layer area conservation and no reactivation of the inherited Mizoën normal fault.

The Oxfordian (upper Jurassic) shales observed at Le Grand Renaud (Fig. 2) were likely also present in the synclines although now eroded away. This weak layer may have allowed decoupling of the Dauphinois cover from the younger Mesozoic series and the internal units: the PFT has thus been drawn much less folded than

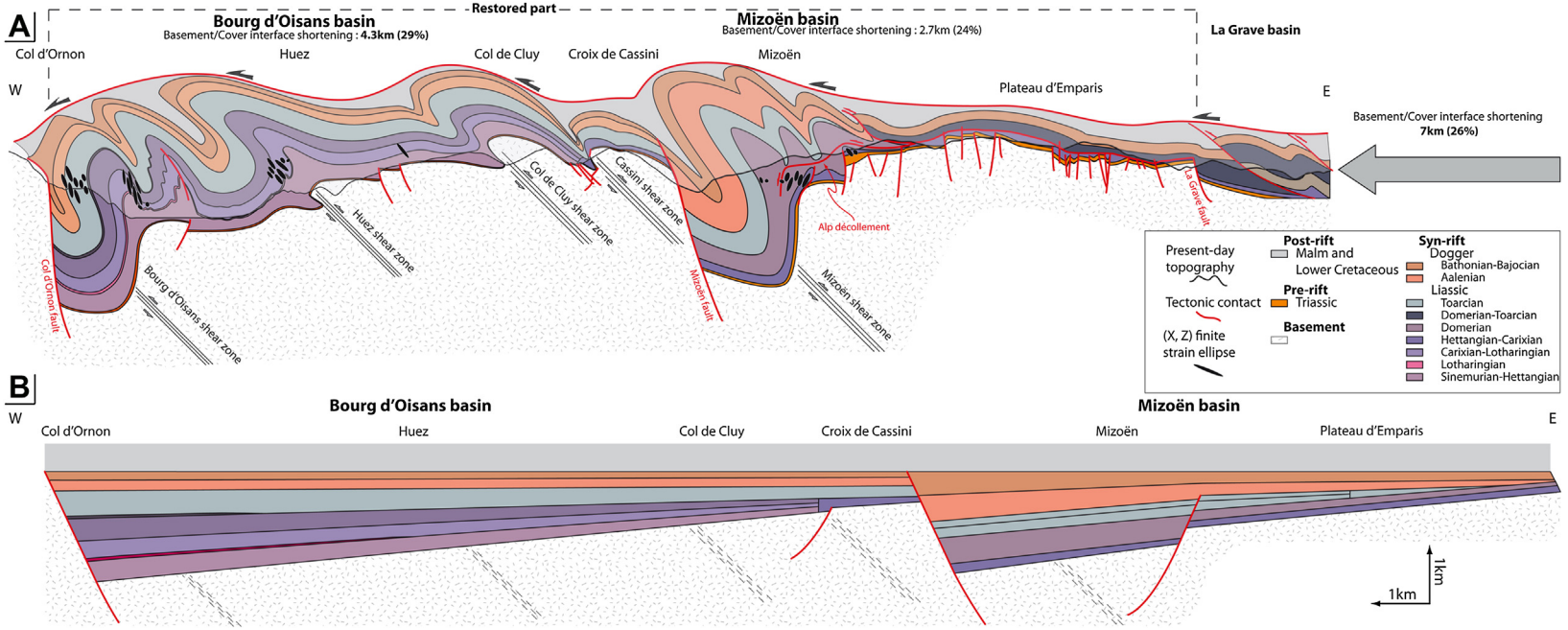

Fig. 4. A: New balanced cross-section of the Bourg d'Oisans and Mizoën basins after field data and geological maps (Barféty et al., 1972; Barbier et al., 1973). B: Restored cross-section. The Mizoën basin was restored with area conservation of the cover. See Fig. 5 for the Bourg d'Oisans hypothesis of restoration.

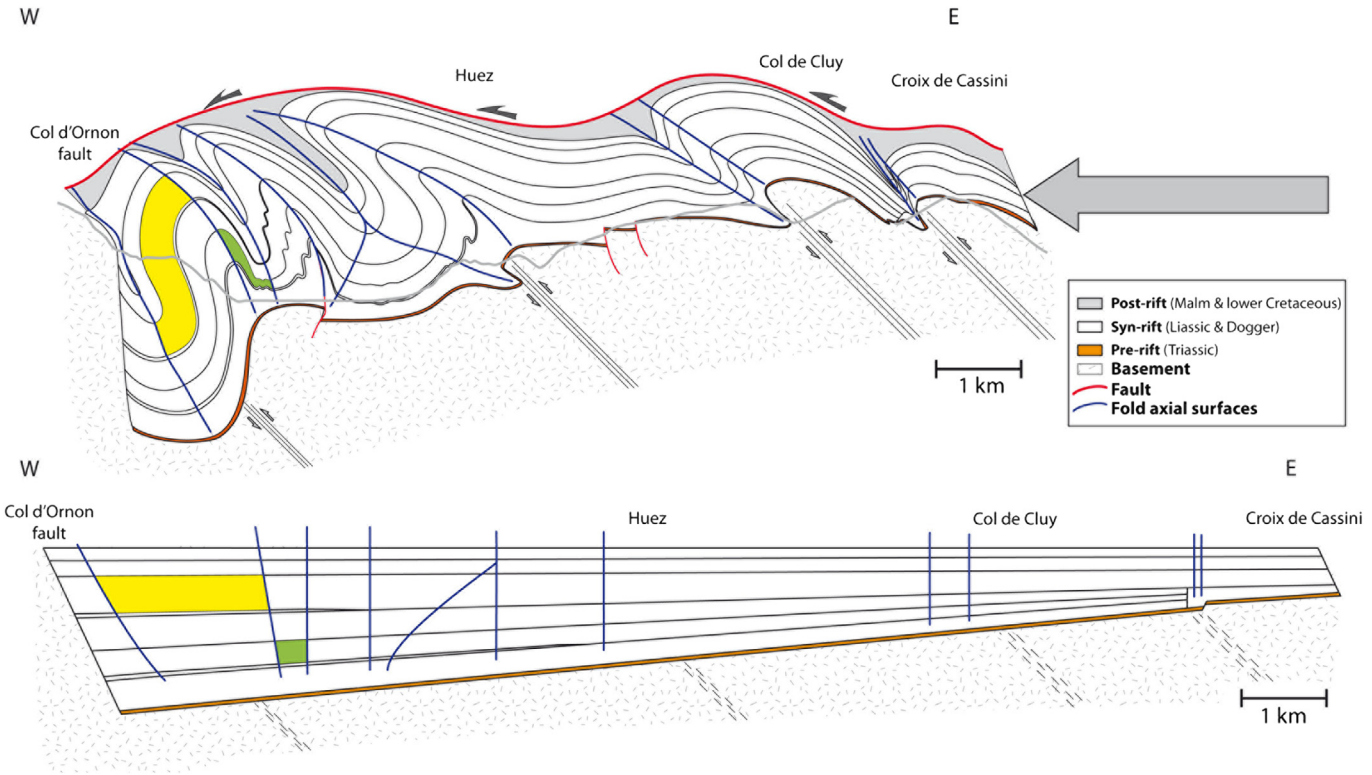

Fig. 5. Restoration of the Bourg d'Oisans basin. The restoration was built assuming: (1) area conservation for the entire cover (the syn-rift sediments) and for each cell defined by bedding and fold axes, (2) conservation of the Triassic basement–cover interface length, (3) no reactivation of the normal faults dipping 65°E, and (4) a dip of 5.5°E for the Triassic.

the underlying rocks (Fig. 4A). This drawing implies that basement shortening and basin inversion were coeval with the PFT activation or at least started during this thrust activity.

4. Outcrop-scale and micro-scale structural analysis

4.1. Cleavages and lineations

In the Bourg d'Oisans basin, two main cleavages, S1 and S2, have been documented in the field (Figs. 6 and 7). Chronological relationships can be deciphered close to the basement, for example near Huez (Fig. 2). Fig. 6 shows an East-verging fold with an axial surface parallel to the early cleavage (S1) which is oriented nearly N–S and oblique to bedding (S0). This likely witnesses a top-to-the-East shearing event of the cover. The vergence of this local shearing during early crustal shortening was probably controlled by the West-dipping top basement surfaces within the inherited tilted blocks.

S1 cleavage predates an East-dipping S2 cleavage consistent with cover folding, itself consistent with a top-to-the-West shearing. It is noteworthy that the S1 cleavage can be observed only near the basement (Fig. 7). The second S2 cleavage is observed all over the basin. It is oriented parallel to the main fold axial surfaces, i.e., N–S and sub-vertical to East-dipping (Fig. 7). Associated to this S2 cleavage, stretching lineations strike mainly E–W, with a scatter from 060°E to 120°E (Fig. 7). They are steeply East-plunging in the western part of the basin, where the cleavage is itself steep and associated to steep fold axial surfaces.

In the Mizoën basin, both cleavages can also be observed. S1 cleavage can be documented only below the Alp décollement (Fig. 8); it is a steep, West-dipping cleavage consistent with the East-verging folds affecting the lower Liassic layers above the hidden basement shear zones (Mizoën shear zone) (Figs. 4 and

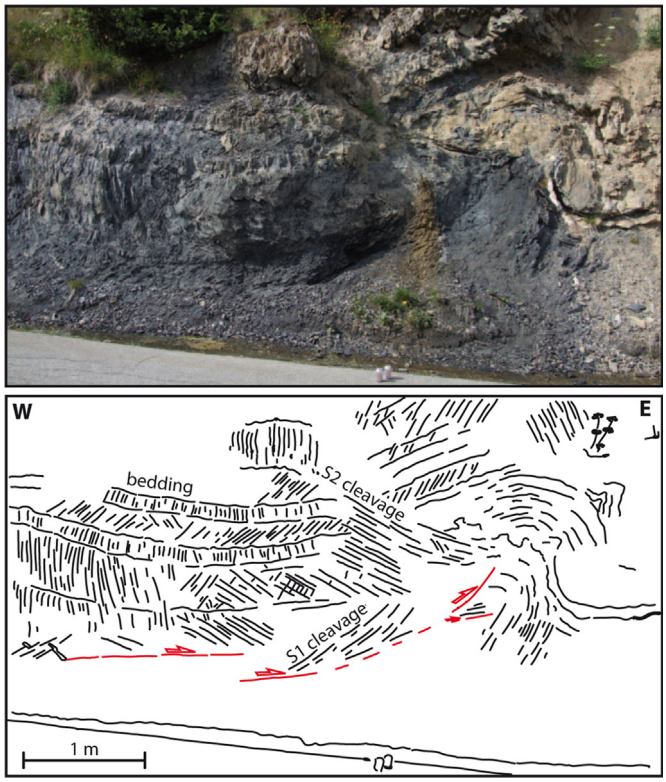

Fig. 6. Chronological relationship between S1 and S2 near Huez (see location on Fig. 2). Modified after Bellahsen et al. (2012). The fold axial surface is parallel to the S1 cleavage. S1 cleavage thus probably results from an East-verging shearing of the cover. The S2 cleavage postdates the S1 cleavage and is parallel to the axial surfaces of the large folds of the cover.

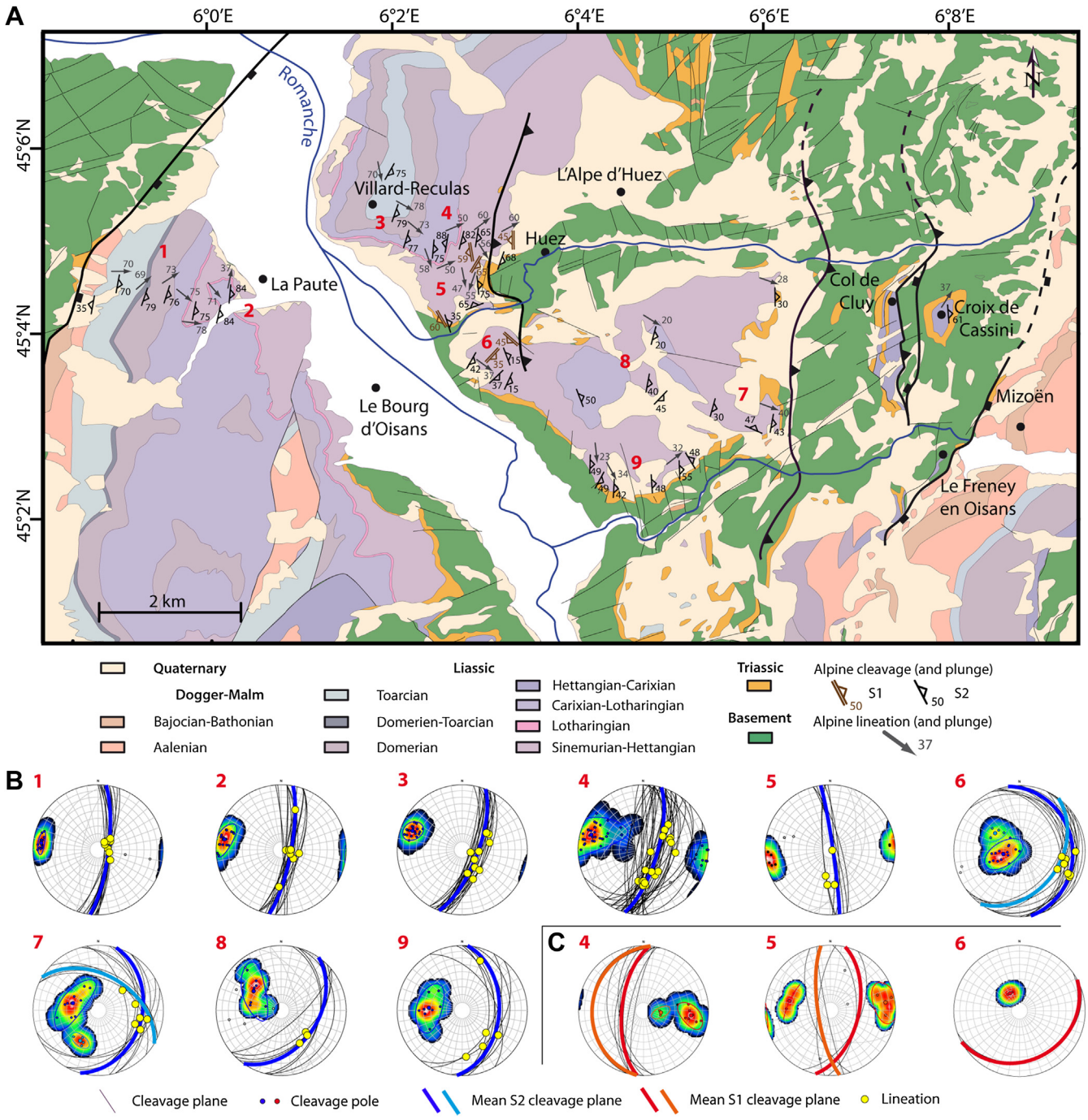

Fig. 7. (A) Alpine cleavages and lineation in Bourg d'Oisans basin. The geological map is modified after Barféty et al. (1972). Two N–S Alpine cleavages (S1 and S2) are observed in Liassic rocks. S2 is usually either vertical or steeply dipping East. (B) Alpine S2 cleavage in the sedimentary cover and lineation (L2) on it. The cleavage and the lineation are mainly dipping toward the East, the cleavage dip decreases from West to East (C). Alpine S1 cleavage can be observed close to the basement, especially West of the Huez shear zone. Because S1 is overprinted by S2 cleavage, lineations on S1 (L1) were not observed.

8). S2 cleavage is absent below the décollement. Above the décollement, however, only the N–S East-dipping S2 cleavage is observed (Fig. 8). It is parallel to the main fold axial surfaces and is thus considered as equivalent to the S2 cleavage of the Bourg d'Oisans basin. On this cleavage, the stretching lineation is trending NE–SW to E–W and is plunging Eastward (Fig. 8). It is noteworthy that toward the basement, the lineation trend becomes closer to N–S.

Small-scale folds can be observed in the field: their axial plane is parallel to the N–S S2 cleavage and their axis is parallel to the stretching lineation on S2. Thus, they are interpreted as witnessing a strong stretching associated with the E–W shortening.

4.2. Cover veins

Calcite/quartz veins are found in many places in the cover. Two types of vein/cleavage chronological relationships have been recognized: veins cutting across cleavages are interpreted as postdating them; conversely, veins that are either transposed and stretched within the cleavage or folded with axial surfaces parallel

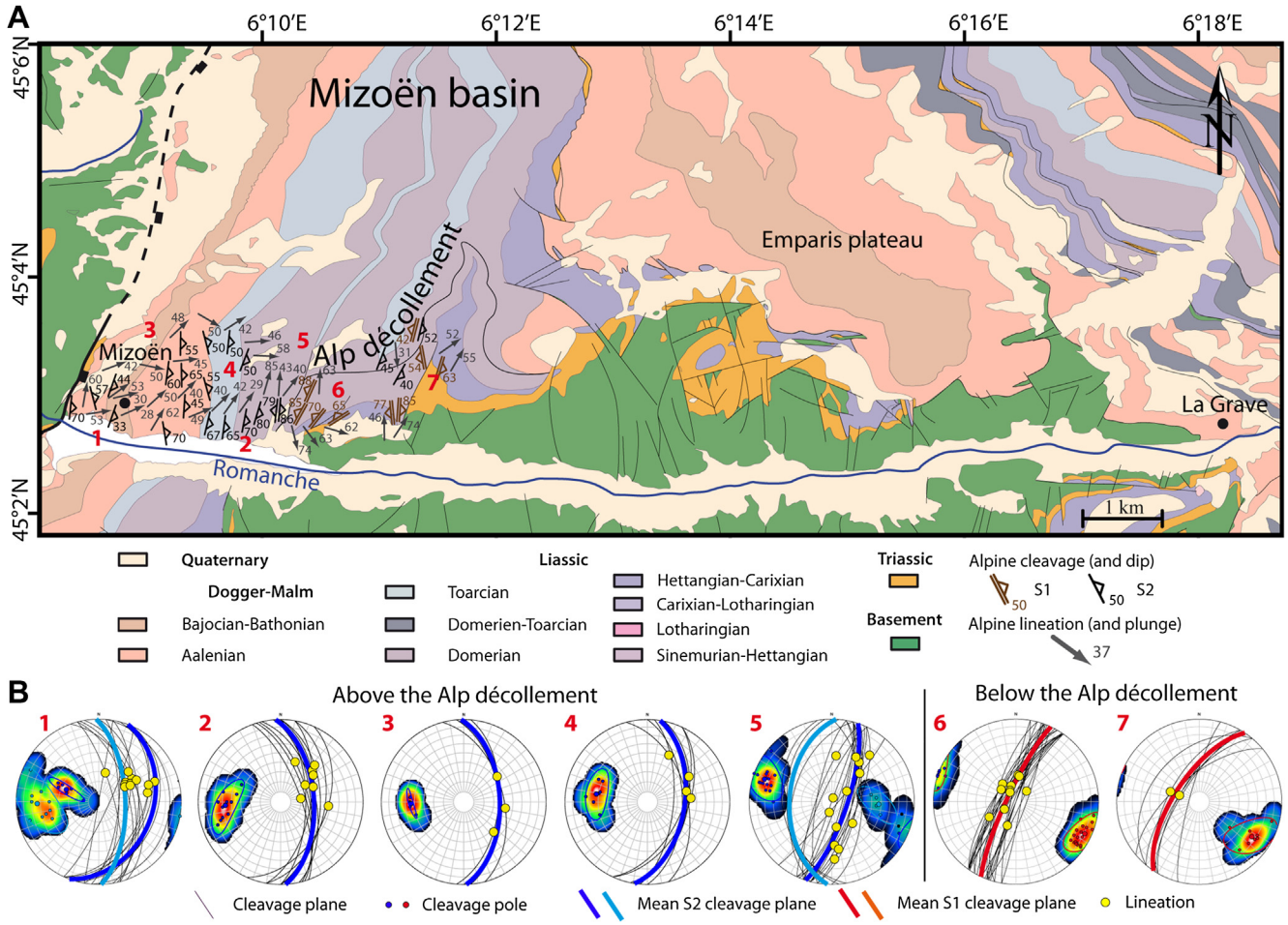

Fig. 8. (A) Alpine cleavages and lineation in Mizoën basin. The geological map is modified after Barbier et al. (1973). Two Alpine cleavages (S2 and S2) are documented in the Liassic rocks. S1 cleavage is restricted to the area close to the basement–cover interface, under the Alp décollement, and generally West-dipping. The S2 cleavage is observed above the Alp décollement and is East-dipping. (B) Alpine S2 cleavage and lineation (L2) on it at sites 1 to 5. The cleavage is mainly dipping toward the East; the dip decreases from West to East. The l2 lineation are East-West in the western part of the basin and tend to become NE–SW and less steep from West to East. The S1 cleavage and lineations (L1) on it are restricted to the structural unit below the Alp décollement is mainly west-dipping and very steep. They are at sites 6 and 7.

to the cleavage (ptygmatic folds) are interpreted as predating cleavage development.

In the Bourg d'Oisans basin, where two main cleavages are observed in the same sites, three sets of veins can be distinguished. V1 veins are deformed by S1 cleavage (Fig. 9D). V2 veins are deformed by S2 cleavage (Fig. 9A) and cut across both S1 cleavage and V1 veins (Fig. 9D). Finally, V3 veins cut across both S1 and S2 cleavages (Fig. 9B and D). The relative chronology of these three vein sets is summarized on Fig. 10A.

In the Mizoën basin, where only the S1 cleavage only is documented below the Alp décollement (Fig. 8), only two vein sets can be defined: V2 and V3 veins cannot be discriminated and are therefore denominated simply as "late veins". Fig. 9C and F shows early veins (V1) that are deformed (ptygmatic or transposed) by the S1 cleavage. Conversely, above the décollement where only S2 cleavage has been identified (Fig. 8), V1 and V2 cannot be discriminated: all veins transposed in S2 are thus simply labeled "early veins". The relative chronological relationships between these vein sets in the two structural units are summarized on Fig. 10B.

It is noteworthy that other problems of vein set determination may also arise locally in the Bourg d'Oisans basin, as the S1 cleavage tends to disappear far from the basement. As a consequence, in younger stratigraphic units, V1 and V2 again cannot be distinguished.

4.3. Synthesis and interpretation

The relative chronology of both cleavages and vein sets is represented in 3D views in Fig. 11. This pattern can be explained by the following kinematic scenario (Fig. 11) : (1) The initial geometry consists of two inherited Liassic syn-rift basins (the Bourg d'Oisans and Mizoën basins, Fig. 11A). (2) During the early stage of E–W shortening, the inherited West-dipping basement–cover interface controlled the deformation kinematics and caused East-verging shearing and development of S1 cleavage (Fig. 11B). Meanwhile, veins consistent with this top-to-the-East shearing initiated with an eastward dip. Close to the main Jurassic faults, shearing is instead top-to-the-West (Fig. 11B). (3) During ongoing shortening, V1 veins were continuously formed and progressively either deformed as ptygmatic veins or transposed by the development of the S1 cleavage (Fig. 11C). At the end of this stage, the latest veins were not deformed by S1 and may thus be recognized in the field as V2 veins. (4) Finally, S2 cleavage started to develop during the West-verging shearing and deformed these former V2 veins (Fig. 11D). The S2 cleavage is synchronous with the top-to-the-West shearing. Successive V2 veins formed during this whole stage and were either transposed or deformed as ptygmatic veins depending on their initial dip angle with respect to the cleavage S2. It is noteworthy that in the field, where the strata are overturned and S1

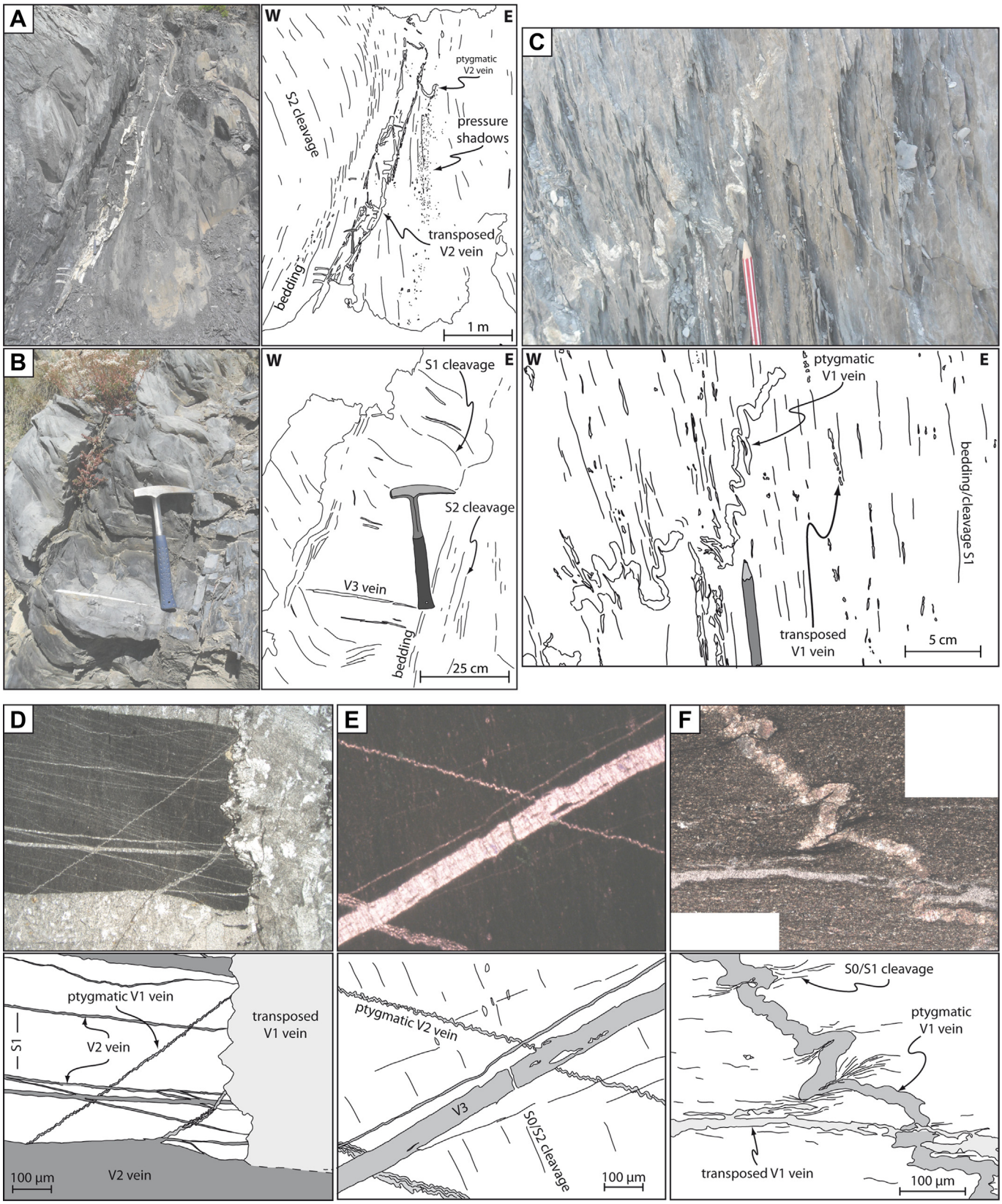

Fig. 9. Veins from the Bourg d'Oisans and Mizoën basins observed at the outcrop or in thin section: (A), (B), (D) and (E) Near Huez village (C) and (F) near Mizoën, under the Alp décollement (see locations on Fig. 2). (A) Transposed V2 vein and S2 cleavage. (B) Late V3 vein compatible with the S2. (C) Ptygmatic vein (V1), S1 cleavage parallel to fold axial surface and V1 vein transposed in the S1 cleavage. (D) Thin section of V1 vein transposed in the S1 cleavage, ptygmatic V1 veins with S1 cleavage parallel to their axial surface and V2 veins cross-cutting the V1 veins. (E) Thin section of ptygmatic V2 veins with S2 cleavage parallel to their axial surface and late V3 veins cross cutting the S2 cleavage and the V2 veins. (F) Thin section of transposed V1 vein in the S1 cleavage and ptygmatic V1 veins with S1 cleavage parallel to their axial surface.

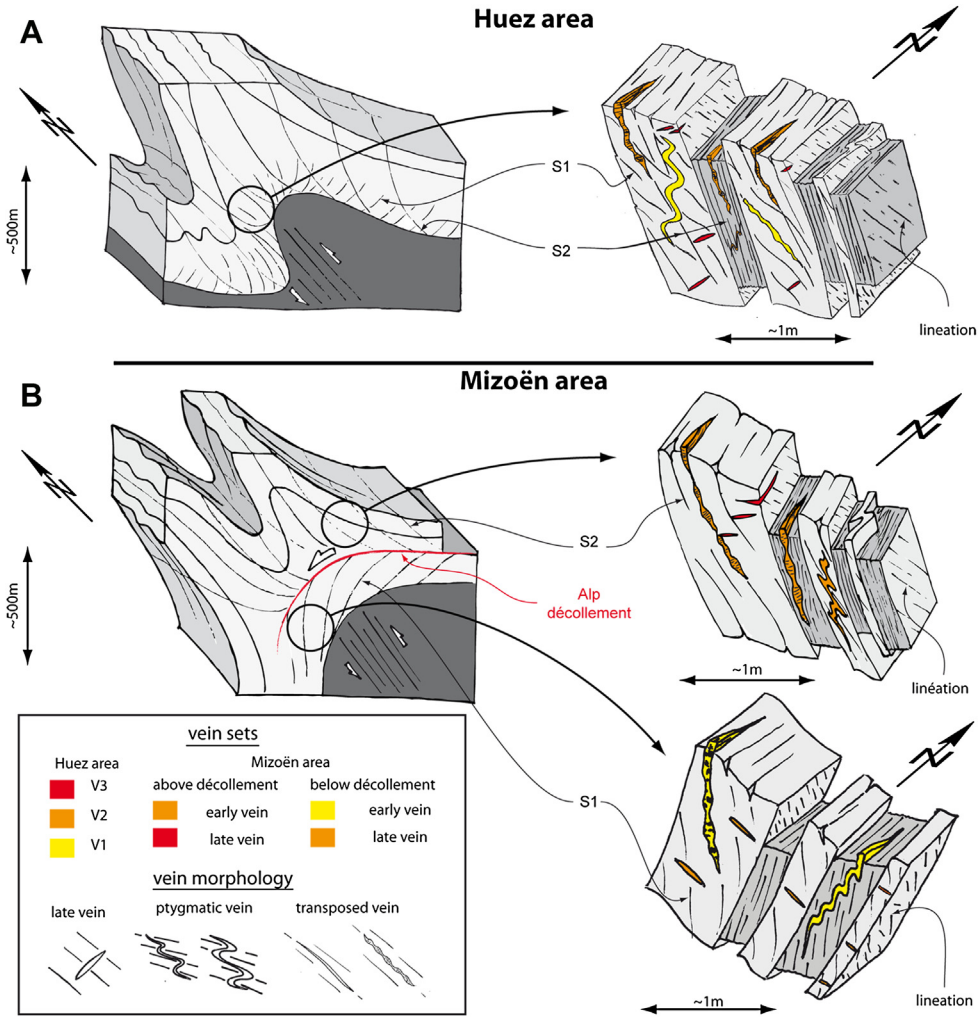

Fig. 10. 3D views of the geometric relationships between the two sets of cleavage and the three sets of veins from field data. In the Bourg d'Oisans area, close to the basement, the two sets of cleavage (S1 and S2) are present. V1 veins are deformed (transposed or ptygmatic) by S1; V2 veins are deformed by S2 and cutting across S1. V3 are non-deformed veins cutting across S1 and S2. In the Mizoën area, under the Alp décollement, only one cleavage associated with west-verging shearing is observed. This is considered as S1 cleavage. Veins deformed by S1 cleavage are early veins (V1) whereas veins cutting across S1 cleavage are late veins (V2/V3). Above the décollement, there is only one cleavage, East-dipping and parallel to the axial plane of overturned folds. This is considered as S2 cleavage. Veins deformed by cleavage are early veins (V1/V2) veins whereas veins cutting across S2 cleavage are late veins (V3).

and S2 sub-parallel, V1 and V2 cannot be discriminated (see Fig. 11D). The latest veins formed were not affected by S2, and even cut across S2; they may therefore be recognized as V3 veins.

4.4. Analysis of the layer internal strain

4.4.1. Methodology

If, at large scale, cover deformation is ductile, at small scale (mm to cm-scale) both brittle and ductile deformation can be observed. The development of cleavages is associated with pressure-solution processes (Gratier et al., 1973), along with pressure shadow development around clasts (e.g., belemnite fragments) or blasts (e.g., euhedral pyrites). Stretching and boudinage of belemnites are however brittle processes, associated with calcite, quartz and pyrophyllite recrystallization between the belemnite clasts. In order to quantify finite strain, we adopted the method proposed by Ramsay and Huber (1989), which is based on the deformation of different inherited clasts within the ductile matrix.

To estimate the X/Y ratio (noted R_{XY} in the following, X and Y being the maximum and intermediate axes of the finite strain ellipsoid, respectively), we used feeding burrows, assuming that they were initially horizontal (parallel to the bedding surface) and randomly oriented (Fig. 12A). Because those burrows were filled during sedimentation, they have the same composition than the host rock, hence a similar viscosity. There is therefore no significant underestimate of the finite strain (Ramsay and Huber, 1989). When the layers were deformed during shortening, these burrows were passively reoriented within the cleavage plane (XY) that developed perpendicular to the local shortening. Their mean orientation in the cleavage plane thus indicates the stretching lineation. R_{XY} was determined on fold limbs where cleavage planes are sub-parallel to bedding so that the initial distribution of burrows in the bedding and the cleavage planes were roughly parallel. In order to have a representative angle distribution and mean orientation of the burrows, we measured at least 300 angles in each sample. Following Ramsay and Huber (1989), the R_{XY} histograms were compared with theoretical Gaussian envelopes (Fig. 12A) computed for theoretical R_{XY}^{th} values (ranging from 1 to 5): the best fit gave us the value for R_{XY}.

The R_{XZ} ratio of the finite strain ellipsoid can be directly estimated from the shape of the pressure shadows (Fig. 12B; Etchecopar and Malavieille, 1987; Ramsay and Huber, 1989) and we

assume that it can be extrapolated to the surrounding host rocks. Here, in order to estimate finite strain we measured only the pressure shadows around framboïdal pyrites (Fig. 12B), which are related to bacterial activity during early diagenesis and so recorded the whole tectonic history. Because the R_{XZ} values do not show important variations, we assume that the average of ten pressure shadows by sample confidently constrains the R_{XZ} ratio for a given outcrop.

To fully quantify the strain ellipsoid, we estimated volume changes during shortening. The numerous vein sets observed in the sedimentary rocks (Fig. 9) are mm- to m-scale veins and are not connected over long distances. Therefore, there is no field evidence for large-scale channels allowing large amounts of fluid flow in these rocks. From stable isotope and trace- and major-element analyses, Henry et al. (1996) concluded that there was no large-scale fluid infiltration in similar Dauphinois cover rocks close to La Grave (East of the Mizoën basin, Fig. 2), but only formation-scale fluid circulations. Both isotopic and trace element analyses evidenced an equilibrium between the mineral vein filling and their host-rock, which implies that the vein filling material has a local origin. It was transported from the surrounding host-rock to veins by pressure-solution/precipitation and small-scale diffusion processes (Oliver, 1996; Oliver and Bons, 2001). Therefore, as pressure-solution/precipitation processes cause local mass redistribution only, the volume change (i.e., mass gain or loss) at the outcrop-scale can be neglected. Rock volume change may also arise due to metamorphic dehydration reactions during burial. In these cover marls, modal calculations (from XRD and bulk rock ICP-AES analysis) show that the pelitic fraction is highly variable, from 0 to about 50 wt.%. Considering that, in the protolith, this pelitic fraction was composed of hydrated clay minerals, the estimated reaction volume (ΔV) is negligible ($\pm$ 2% maximum) and the mineral volume change due to metamorphic dehydration reactions may not exceed a few percents: a maximum of 8% can be calculated for a highly pelitic sample. Thus, it is reasonable to assume that there was no or very few volume change at the outcrop-scale (i.e., meter-scale) in the cover rocks during deformation.

With R_{XY}, R_{XZ} ratios and the constant volume hypothesis, the absolute values of the X, *Y* and *Z* axes of the finite strain ellipsoid were computed, as long as R_{XY} and R_{XZ} were measured on the same outcrop (Fig. 12C).

4.4.2. Field data

The R_{XY} and R_{XZ} ratios were measured in the field along the E–W cross-section in the Bourg d'Oisans basin: above the Bourg d'Oisans shear zone (17 ellipsoids) and above the Huez shear zone (12 ellipsoids) (Fig. 4). The ellipsoids were also reconstructed in the Mizoën basin, along a transect above the Mizoën shear zone (12 ellipsoids) (Fig. 4). Each ellipsoid was computed and then projected as an apparent (XZ) ellipse on the cross-section plane (Fig. 4).

In the cover fold above the Bourg d'Oisans shear zone, the (*XZ*) ellipse distribution shows few variations. The R_{XZ} ratios are mainly between 3 and 4, with two exceptions: two R_{XZ} ratios of 1.5 on the eastern side of the fold (Fig. 4). This variation does not indicate a local strain decrease but are due to a local change of lineation orientation (Fig. 7, on the western side of "La Paute" village). Above the Huez shear zone, the (*XZ*) ellipse shape seems to be more variable, although constant in orientation. This variability could be related to second-order folding (Fig. 4).

In the Mizoën basin, we observe a change in the (*XZ*) ellipse dip across the Alp décollement, which is consistent with the change in cleavage dip: above the décollement, the ellipses are East-dipping like S2, whereas below the décollement, the ellipses are West-dipping like S1. The apparent increase in the (XZ) ellipse elongation from the Alp décollement ($X/Z = 1$) to the basement ($X/Z = 3.5$) is due to the projection of the ellipsoids on the cross-section, because the lineation trend is N–S close to the décollement and progressively turns to E–W below it (Fig. 8).

5. Discussion

5.1. (Micro)-structural evolution

In the Bourg d'Oisans basin, an S1 cleavage developed during a transient event of top-to-the-East shearing only close to the basement–cover interface. This cleavage is overprinted by the main (S2) cleavage that affected the whole cover. In the Mizoën basin, the presence of the Alp décollement apparently spatially segregated the two cleavages: the S1 cleavage is mainly located below the décollement while the S2 one is restricted to the upper unit. This suggests that the lower unit has been less affected by the shortening and shearing phase that formed the S2 cleavage. Conversely, above the décollement, the S1 cleavage is absent because the layers were too far from the basement–cover interface to be affected by the local top-to-the-East early shearing.

Both cleavages can thus be explained by a continuum of deformation during E–W shortening that corresponds to the D3 phase in Dumont et al. (2008, 2011). Their spatial variability is strongly linked to the larger-scale deformation and, in particular, to the structural style.

5.2. Robustness of restorations

In order to check the robustness of the Bourg d'Oisans basin restoration, we computed the initial bottom and top length for two cells using the (XZ) finite strain ellipses. A similar approach was followed by Yakovlev (2012). Here, we reduce of *x* times cells bottom and top lengths of the Bourg d'Oisans cross-section, where *x* is the absolute extension value (*X* axis on strain ellipsoids) previously computed (see Fig. 13A for the location and Fig. 13B for comparison). Then, we compare those "inverted" lengths to the bottom and the top lengths of the restored cells (see Fig. 13A for the construction and the location of cells and Fig. 13B for comparison).

The computed (*XZ*) ellipses have similar ranges of shape (extension from 1.5 to 2.5 along *X* and about 0.45 along *Z*) (Fig. 4A). These ellipses result from the interpretation of various objects widespread within several samples for each outcrop, and thus are confidently representative of internal strain at the outcrop scale.

The comparison of bottom and top lengths of our restored cells with the lengths restored with the (*X*,*Z*) ellipses inversion (Fig. 13B) shows a good fit, except for the top of the cell 1. It suggests that the balancing of the Bourg d'Oisans cross-section is correct because the two methods of cell restoration are in agreement. Furthermore, it shows that one may reliably restore any major fold of a basin cover without using the basement–cover interface, but only by considering the cover layer surfaces and their internal finite strain.

In the western part of the La Paute fold however, the cell 1 (Fig. 13B) is geometrically balanced (the area conservation requirement is fulfilled) but the top cell length deduced from the strain ellipsoid data does not fit exactly the one given by the restoration. One solution to solve the problem would be to deepen the Col d'Ornon syncline and so the pinching of the Bourg d'Oisans basin or to move up the top of the La Paute anticline. But it would imply to strongly increase the size of the La Paute anticline limb (yellow, in the web version cells on Fig. 13) and move up its hinge. This also implies to strongly thin the limb, as the cell areas are constant. However, the limb widths are constrained by field data and geological maps. Thus, the misfit between restoration approaches cannot be easily solved. More strain ellipsoids are probably needed to precisely address this discrepancy.

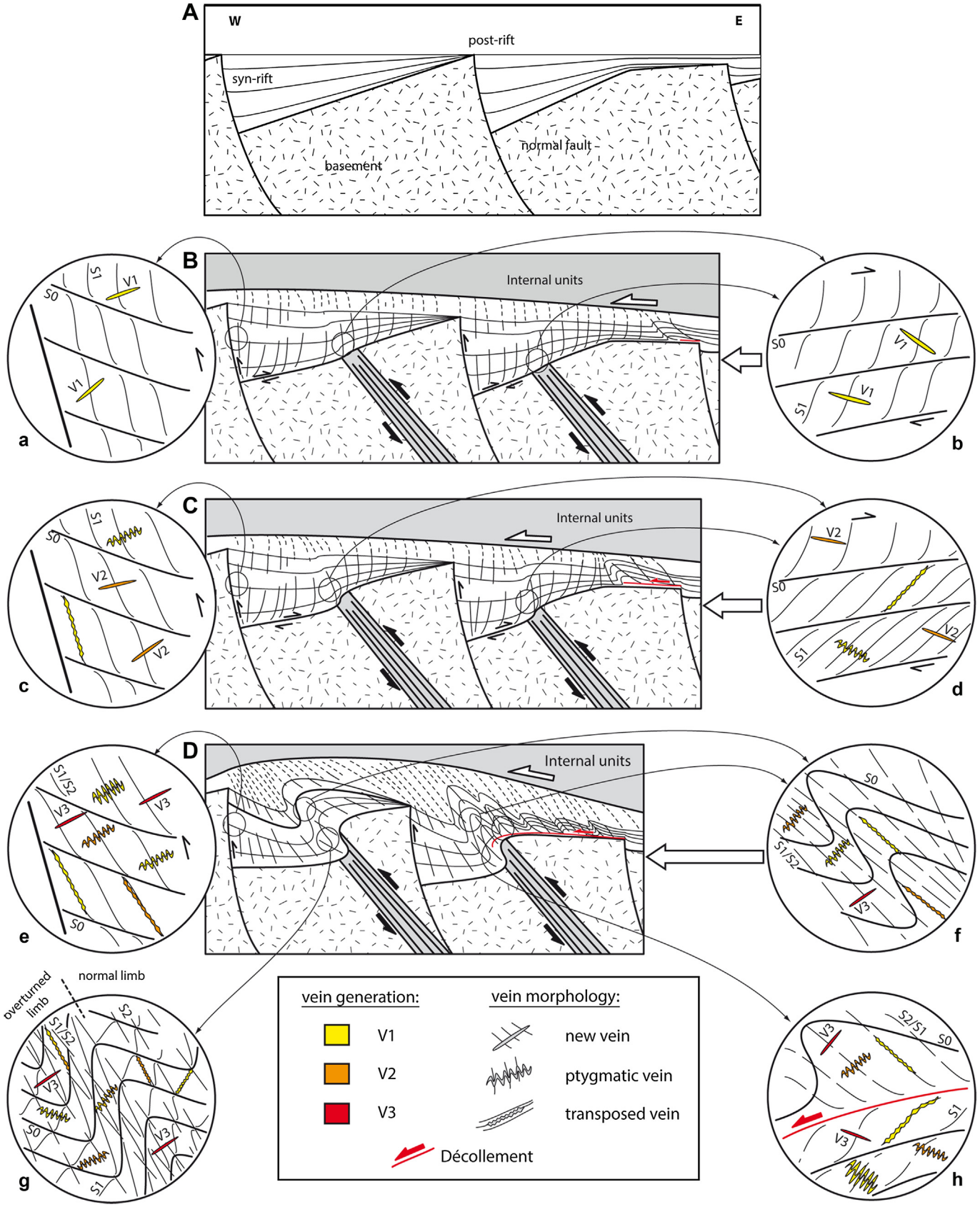

Fig. 11. Kinematic scenario of cleavage and vein development in the cover. A) Inherited Mesozoic setting. The basins were West-dipping and controlled by East-dipping normal faults. B) First stage of shortening. The cover and the basement began to be folded and a sub vertical cleavage (S1) and V1 veins formed: (a) near the inherited normal fault and (b) at the bottom of the basin (above the Triassic layer). C) End of the first shortening stage: (c, d) as the cover was deformed, veins were continuously formed. The veins with a small initial angle between the vein and the cleavage were progressively transposed into S1 while other ones, with a high initial angle with the cleavage, became ptygmatic. At the end of

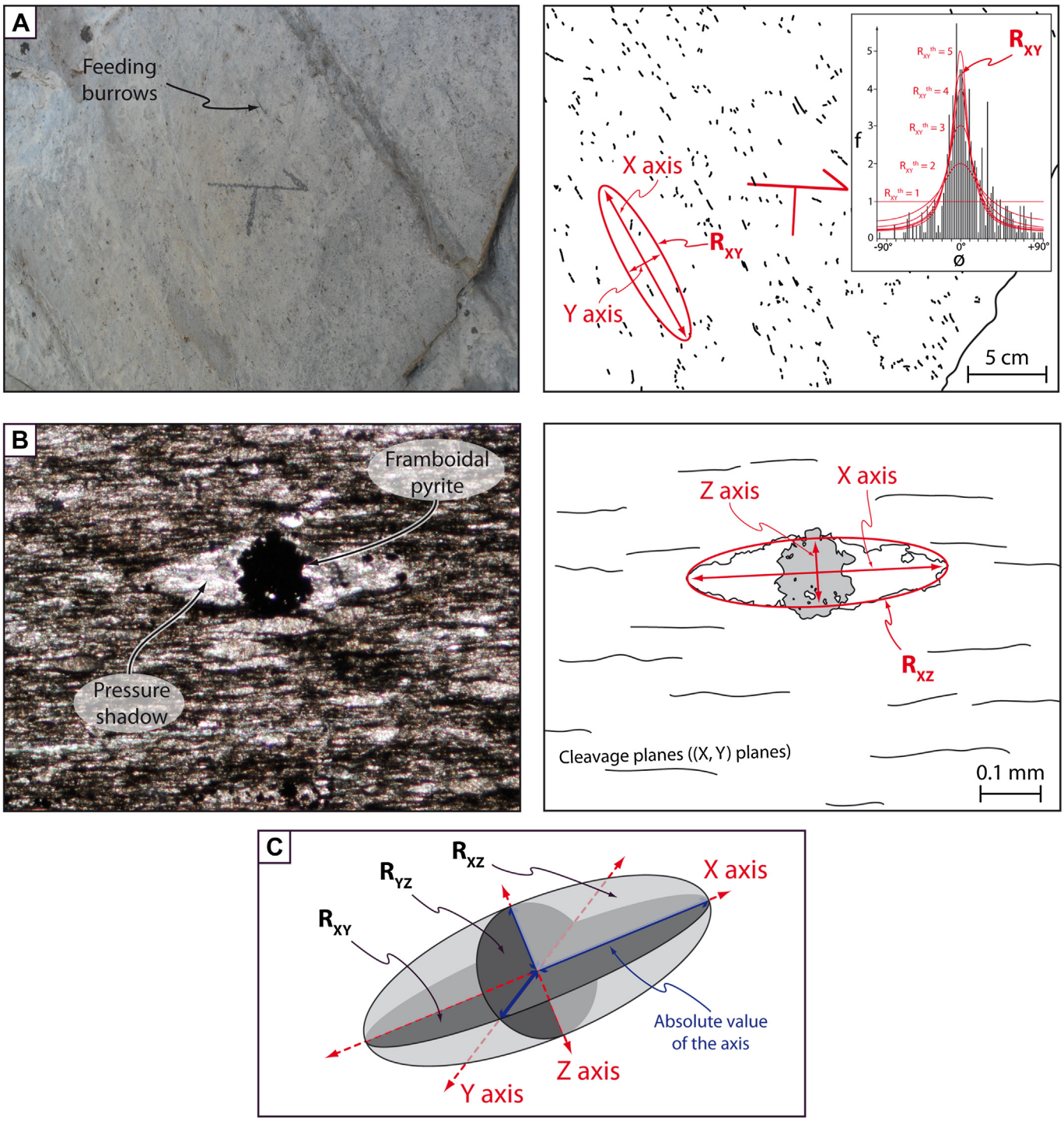

Fig. 12. Methodology of finite strain ellipsoid construction. (A) R_{XY} determination with passive reorientation of feeding burrows around the *X* axis. The angle distribution is compared to a theoretical R_{XY}th plot on the graph (Ramsay and Huber, 1989). On the displayed example, 528 feeding burrows were measured and $R_{XY} = 4.5$. (B) R_{XZ} determination with direct estimation from framboidal pressure shadow shape (Etchecopar and Malavieille, 1987; Ramsay and Huber, 1989). Here $R_{XZ} = 3.8$.

the East-verging shearing phase, V2 veins were formed, not deformed by S1 but only by S2. D) A second phase of shortening, still contemporaneous with basement shearing, strongly deformed the cover. Various configurations can be found depending on the structural location in the basin. Close to the normal faults (e) and in the basin center (f), cleavage (S1/S2) kept forming during shearing or folding (S1 and S2 cannot be distinguished). V2 veins are still forming and deformed (V1 and V2 cannot be distinguished). (g) Close to the bottom of the basins, west-verging shearing and associated S2 cleavage overprinted East-verging shearing and associated S1 cleavage. S2 was parallel to the axial surface of the folds whereas S1 was deformed. In overturned limbs, S1 and S2 were sub-parallel and cannot be distinguished. In normal limbs, S1 and S2 show a high angle and allow the distinction between V1 and V2. (h) Where the cover was detached from the basement, there was no overprinting of the cleavage and S2 was developed only above the décollement. V1 and V2, as well as V2 and V3, cannot be distinguished above and under the décollement, respectively. V3 were formed at the end of west-verging shearing phase and were not deformed by S2.

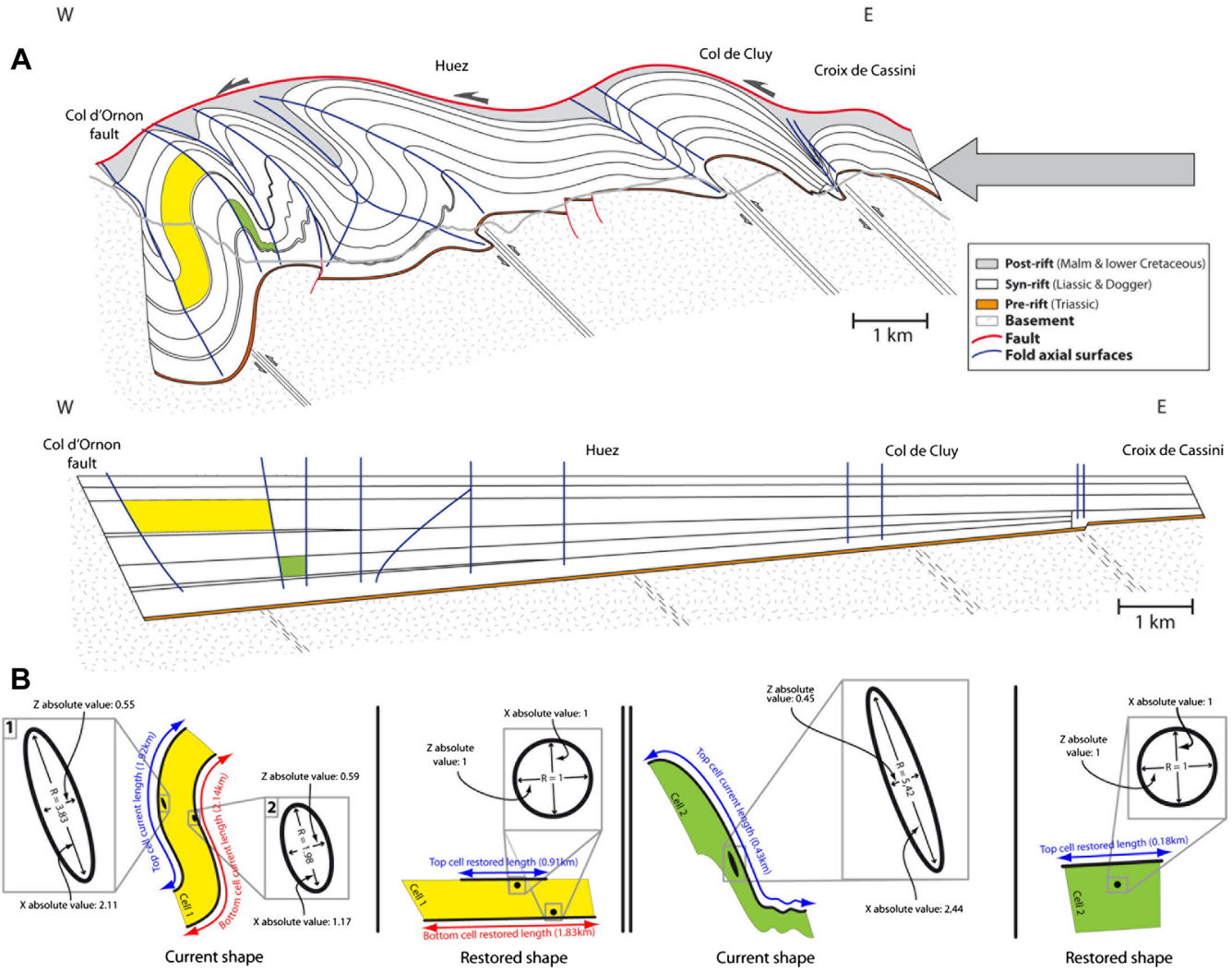

Fig. 13. Restoration of two cells from the Bourg d'Oisans cross-section. The cells are limited by stratigraphic boundaries and fold hinges, in the western part (cell 1) and in the eastern part (cell 2). The presented ellipses are representative of 9 ellipses for cell 1 and 8 ellipses for cell 2. The restorations are performed with constant area hypothesis (yellow and green cells) and with the (XZ) finite strain ellipses inversion method (blue double arrows). [For interpretation of color referred in this figure legend, the reader is referred to web version of the article.]

5.3. Structural evolution and amount of shortening in the Oisans massif

The fold wavelength in the Mizoën basin (~1 km) is shorter than in the Bourg d'Oisans (~2 km) (Fig. 3). This is likely due to the décollement in the Mizoën basin (Alp décollement; Fig. 3). The different structural styles (décollement in the Mizoën basin vs no significant décollement in the Bourg d'Oisans basin) may be linked to the amount of basement shortening in the Mizoën basin (2.7 km) which is lower than in the Bourg d'Oisans basin (4.3 km). The weakening effect of the thick syn-rift series (up to 3 km) in the Bourg d'Oisans basin may have promoted basement shortening, hence precluding significant cover décollement, whereas the wide weakly thinned crustal domain of the Emparis Plateau was less shortened and therefore likely more prone to deform in a thin-skinned style with décollement of the thin cover (Bellahsen et al., 2012). Note that this difference in amount of basement shortening and structural style, which is controlled by the geometry and subsidence of pre-orogenic extensional basins, controls the microstructural evolution and the spatial segregation of cleavages, the S2 cleavage in the cover of the Mizoën basin being restricted to the detached part of the cover while the lower unit below the decollement only shows evidence of S1cleavage.

5.4. Shortening in the External Crystalline Massifs

In Liassic times, the European crust was stretched and structured in tilted blocks. In Tertiary times, this crust was subsequently deformed in two steps. First, the distal parts were subducted and formed the so-called internal units. Later, the proximal parts were buried under the internal units and formed the external zone (Fig. 14A and B). Along the strike of the Alpine ECM, the burial conditions of the proximal part increased from South (2–3 kbar, 300 °C in the Oisans, Crouzet et al., 2001; Simon-Labric et al., 2009) to North (5 kbar, 450 °C in the Mont Blanc, Rolland et al., 2008). The cover of the northern massifs (e.g., Mont Blanc) is highly deformed and slightly detached and translated from its basement (Morcles nappe, Figs. 1 and 14). As a consequence, its restoration is still debated even though most authors, except Leloup et al. (2005), suggest that the Morcles nappe corresponds to the former Mont Blanc cover (e.g. Escher et al., 1993; Burkhard and Sommaruga, 1998). There is also a debate in the literature concerning the

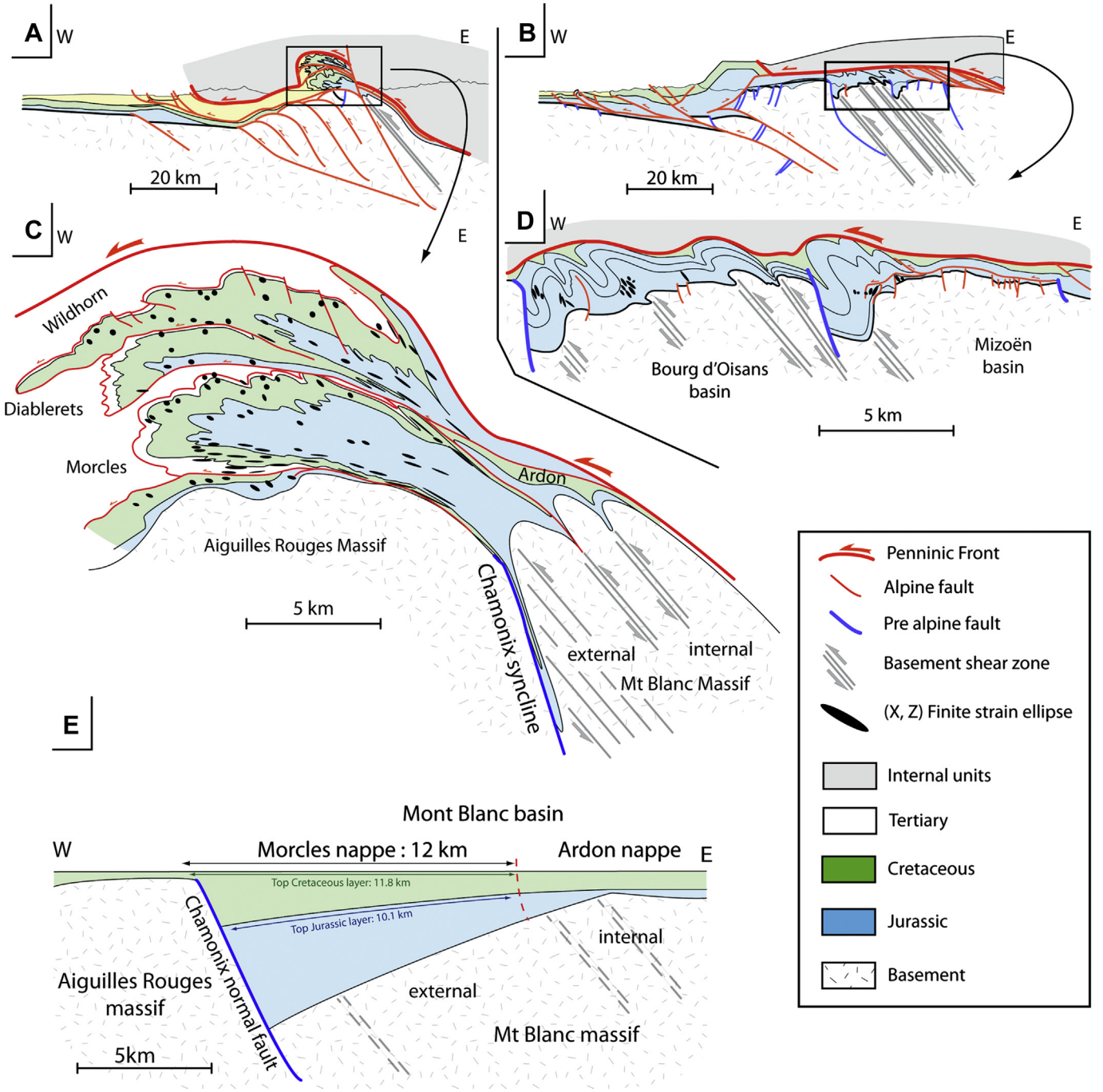

Fig. 14. Cross-sections of the external zone and ECM. A) External zone in the Mont Blanc area, modified after Burkhard and Sommaruga (1998). B) External zone at the North Oisans latitude, modified after Bellahsen et al. (2012). C) Cross-section of the ECM and (XZ) finite strain ellipses at the Mt Blanc latitude, modified after Ramsay et al. (1983) and Escher et al. (1993). D) Cross-section of the ECM and (*XZ*) finite strain ellipses at the North Oisans latitude (this study). (E) Restoration of the Morcles nappe based on cover area conservation hypothesis and (*XZ*) finite strain ellipse inversion.

Ardon nappe, located East of Morcles nappe : still attached to the internal Mont Blanc massif (Escher et al., 1993) or detached and carried on the Mont Blanc massif (Burkhard and Sommaruga, 1998). In the following, the Morcles and the Ardon nappes are compared to the deformed metasedimentary cover of the Oisans massifs.

We here assume that the Morcles and the Ardon nappes (Fig. 14C), now located above the Aiguilles Rouges massif, represent the former sedimentary cover of the external and internal Mont Blanc basement, respectively (Escher et al., 1993). The Morcles nappe is a recumbent fold, consisting primarily of Jurassic and Cretaceous limestones. At its base, the shear zone roots in the Mont Blanc massif (Pfiffner, 1981; Ramsay, 1981; Escher et al., 1993). The Morcles nappe was the cover of a tilted block in which sedimentation was probably controlled by the Chamonix normal fault, although the latter does not clearly crop out in the Chamonix syncline (Burkhard and Sommaruga, 1998). The basement of the Mont Blanc massif is strongly sheared (Mont Blanc shear zone, Leloup et al., 2005; Rolland et al., 2008). This resembles our Oisans cross-section where the basement of inherited Jurassic basins is strongly sheared (Fig 14D). The Morcles nappe and the Mont Blanc basement may thus be considered as analog to the basement-cover system observed in the Oisans massif, where the cover is disharmonically folded above

basement shear zones. However, in the Mont Blanc, both the shortening and the P–T conditions were significantly higher (Poty et al., 1974; Hoschek, 1980; Rolland et al., 2008), which makes the structural interpretation more complicated than in the Oisans even though the structural style is basically the same.

The cross-section in the northeastern Mont Blanc massif was balanced by Burkhard and Sommaruga (1998; Fig. 14A) with constant length for the Triassic layers and constant area for the overlying Mesozoic metasedimentary formations. Here, we tentatively restore the Morcles nappe using only the internal strain field characterized by the available strain ellipses (Ramsay, 1981; Ramsay and Huber, 1989): in other words, the basement–cover interface geometry and length were not taken into account. The goal is to test if such restorations can be performed for a ductilely deformed unit and with no or few constraints on the basement–cover interface geometry. We used the (*XZ*) ellipse data (Ramsay and Hubert, 1989) on a section (Fig. 14C) modified after Escher et al. (1993) to determine the restored length of the top of two specific layers, namely the Cretaceous and the Jurassic. The section was modified as follows: the Chamonix normal fault has been added with an initial dip of 65°. The Chamonix syncline has thus been drawn very pinched. We assume that the normal fault was not reactivated. The restoration was performed with constant area for the cover layers.

This new restoration of the Morcles nappe was performed in two successive steps. First, we inverted the (XZ) ellipse data of Ramsay and Huber (1989) to obtain the initial length of the top of Cretaceous and Jurassic layers. The ellipses are not perfectly homogeneously distributed within the nappe. Thus, we cannot assess the variability of layer internal strain for each fold (Ramsay and Huber, 1989). A second problem is that (XZ) ellipses are available neither for the Chamonix syncline nor for the eastern normal limb of the Morcles nappe (Fig. 14C). For those two places, we chose to extend the value of the easternmost ellipses towards the East. Because these ellipses are extremely long (the X/Z ratio is about 20 in the inverted limb and about 10 in the normal limb), the corresponding restored lengths are very short.

The second step of the restoration is the area conservation for the nappe layers along the cross-section plane. Because the top of the Cretaceous and the top of the Jurassic lengths (11.8 and 10.1 km, respectively) are fixed by the previous step, the area constrains the inherited normal fault displacement and so the depth of the half-graben, which is here about 6 km (Fig. 14).

Finally, from the restored geometry of the Morcles nappe fixed by the previous steps, we restored the Ardon nappe on the eastern part of the half graben. The restoration was done with constant area hypothesis for the Jurassic and Cretaceous layers and the thickness was constrained by the thickness of the restored Morcles nappe along its eastern boundary (Fig. 14E).

The restored length of the Morcles nappe is about 12 km, which represents the western part of a half-graben, the Mont Blanc basin. This basin includes the restored Ardon nappe; the total basin length is then about 15 km and the depth about 6 km (Fig. 14E). This result is quite different from the restoration by Burkhard and Sommaruga (1998), as these authors proposed a basin about 24 km long and 2 km deep. Even though the two restorations are both based on area conservation, our restoration reveals a pre-orogenic graben structure which is narrower but twice deeper than that in Burkhard and Sommaruga (1998). These authors preserved the Triassic length in order to restore the basement top: however, this layer has probably been strongly stretched above the numerous basement shear bands of the Mont Blanc shear zone (Leloup et al., 2005; Rolland et al., 2008). This may explain the difference between the two restorations. The Mont Blanc basin size that we obtain implies a very strong increase (of 43% or 6 km) of the length of the basement–cover interface during the inversion of the European margin. Moreover, this increase is more important for the internal part (101% or 4.2 km) than for the external one (18% or 1.8 km). This is consistent with the overturned attitude of the Triassic layers below the Mont Blanc shear zone and their scarce outcrops due to their strong thinning (Mennessier et al., 1977; Antoine et al., 1978; Ayrton et al., 1987).

6. Conclusion

In this contribution, we present balanced cross-sections of the External Crystalline Massifs based on a new approach. Indeed, we show that microstructural studies and quantification of the strain ellipsoid in the cover can help restore areas where strong length changes affected the sedimentary layers. We show that contrasting amounts of shortening affected the different inverted pre-orogenic basins with (micro)structural consequences in terms of cleavage development. In places where the basement was strongly shortened, there is no significant décollement of the cover, whereas such a décollement initiated in places where the amount of basement shortening was lower, and led to a spatial segregation of cleavages within the cover. Such various amounts of collisional basement shortening are probably due to different pre-orogenic extensional geometries/crustal structures: in domains of thick and large syn-rift basins, the crust is weak and a high amount of shortening is recorded; in contrast, in domains with thin syn-rift basins, less crustal shortening is accommodated.

Acknowledgments

The authors would like to thanks Y. Rolland, C. Rosenberg, L. Jolivet and M. Bellanger for discussions and X. and M.O. Gonord for their warm welcome during field trips. Reviews by J.L. Epard and F. Roure greatly improved the original version of the manuscript. This study was funded by the “Syster” INSU program, the BRGM contract L10 U 044, and ISTeP (UPMC) funds.

References

Affolter, T., Faure, J.L., Gratier, J.P., Colletta, B., 2008. Kinematic models of deformation at the front of the Alps: new data from map-view restoration. Swiss J. Geosci. 101 (2), 289–303.

Antoine, P., Féraud, J., Poulain, P.-A., 1978. Carte géologique de la France (1/50.000), feuille du Mont Blanc (704). Bureau de Recherche géologique et miniÀre, Orléans.

Ayrton, S., Barféty, J.-C., Bellière, J., Gubier, Y., Jemelin, L., 1987. Carte géologique de la France (1/50.000), feuille de Chamonix (680). Bureau de Recherche géologique et miniÀre, Orléans.

Barbier, R., Barféty, J.C., Bocquet, A., Bordet, P., Le Fort, P., Meloux, J., Mouterde, R., PÕcher, A., Petiteville, M., 1973. Carte géologique de la France (1/50.000), feuille de La Grave (798). Bureau de Recherches géologiques et minière, Orléans.

Barféty, J.C., Bordet, P., Carme, F., Debelmas, J., Meloux, M., Montjuvent, G., Mouterde, R., Sarrot-Reynauld, J., 1972. Carte géologique de la France (1/50.000), feuille de Vizille (797). Bureau de Recherches géologiques et miniÀres, Orléans.

Barféty, J.C., Gidon, M., Lemoine, M., Mouterde, R., 1979. Tectonique synsédimentaire liasique dans les massifs cristallins de la zone externe des Alpes occidentales françaises: la faille du col d'Ornon. C.R. Acad. Sci. Paris 289, 1207–1210.

Beach, A., 1982. Strain analysis in a cover thrust zone, external French Alps. Tectonophysics 88 (3), 333–346. http://dx.doi.org/10.1016/0040-1951(82)90245-1.

Bellahsen, N., Jolivet, L., Lacombe, O., Bellanger, M., Boutoux, A., Garcia, S., Mouthereau, F., LePourhiet, L., Gumiaux, C., 2012. Mechanisms of margin inversion in the external Western Alps: Implications for crustal rheology. Tectonophysics 560, 62–83. http://dx.doi.org/10.1016/j.tecto.2012.06.022.

Buiter, S.J., Pfiffner, O.A., 2003. Numerical models of the inversion of half-graben basins. Tectonics 22 (5), 1057. http://dx.doi.org/10.1306/06301009165.

Burkhard, M., Sommaruga, A., 1998. Evolution of the Western Swiss Molasse basin: structural relations with the Alps and the Jura belt. In: Mascle, A., Puigdefabregas, C., Luterbacher, H.P., Fernanfez, M. (Eds.), Cenozoic Foreland Basins of Western Europe, Geological Society, London Special Publication, vol. 134, pp. 279–298. http://dx.doi.org/10.1144/GSL.SP.1998.134.01.13.

Butler, R.W.H., 1986. Thrust tectonics, deep structure and crustal subduction in the Alps and Himalayas. J. Geol. Soc. 143 (6), 857–873. http://dx.doi.org/10.1144/gsjgs.143.6.0857.

Butler, R.W.H., 1989. The influence of pre-existing basin structure on thrust system evolution in the Western Alps. Geol. Soc. Lond. Spec. Publ. 44 (1), 105–122. http://dx.doi.org/10.1144/GSL.SP.1989.044.01.07.

Butler, R.W., 2013. Area balancing as a test of models for the deep structure of mountain belts, with specific reference to the Alps. J. Struct. Geol. 52 (13), 2–16. http://dx.doi.org/10.1016/j.jsg.2013.03.009.
Butler, R.W., Tavarnelli, E., Grasso, M., 2006. Structural inheritance in mountain belts: an Alpine–Apennine perspective. J. Struct. Geol. 28 (11), 1893–1908. http://dx.doi.org/10.1016/j.jsg.2006.09.006.
Ceriani, S., Fügenschuh, B., Schmid, S.M., 2001. Multi-stage thrusting at the "Penninic Front" in the Western Alps between Mont Blanc and Pelvoux massifs. Int. J. Earth Sci. 90 (3), 685–702. http://dx.doi.org/10.1007/s005310000188.
Chamberlin, R.T., 1910. The Appalachian folds of central Pennsylvania. J. Geol. 18 (3), 228–251.
Chopin, C., 1987. Very-high-pressure metamorphism in the Western Alps: implications for subduction of continental crust [and Discussion]. Philos. Trans. R. Soc. Lond. Ser. A Math. Phys. Eng. Sci. 321 (1557), 183–197. http://dx.doi.org/10.1098/rsta.1987.0010.
Crouzet, C., Ménard, G., Rochette, P., 2001. Cooling history of the Dauphinoise Zone (Western Alps, France) deduced from the thermopaleomagnetic record: geodynamic implications. Tectonophysics 340 (1), 79–93. http://dx.doi.org/10.1016/S0040-1951(01)00142-1.
Dahlstrom, C.D.A., 1969. Balanced cross-sections. Can. J. Earth Sci. 6 (4), 743–757.
De Graciansky, P.C., Dardeau, G., Lemoine, M., Tricart, P., 1989. The inverted margin of the French Alps and foreland basin inversion. Geol. Soc. Lond. Spec. Publ. 44 (1), 87–104. http://dx.doi.org/10.1144/GSL.SP.1989.044.01.06.
Deville, É., Chauvière, A., 2000. Thrust tectonics at the front of the Western Alps: constraints provided by the processing of seismic reflection data along the Chambéry transect. C.R. Acad. Sci. Sér. II 331 (11), 725–732. http://dx.doi.org/10.1016/S1251-8050(00)01463-4.
Deville, É., Sassi, W., 2006. Contrasting thermal evolution of thrust systems: an analytical and modeling approach in the front of the western Alps. AAPG Bull. 90 (6), 887–907. http://dx.doi.org/10.1306/01090605046.
Dumont, T., Champagnac, J.D., Crouzet, C., Rochat, P., 2008. Multistage shortening in the Dauphiné zone (French Alps): the record of Alpine collision and implications for pre-Alpine restoration. Swiss J. Geosci. 101 (1), 89–110. http://dx.doi.org/10.1007/978-3-7643-9950-4_6.
Dumont, T., Simon-Labric, T., Authemayou, C., Heymes, T., 2011. Lateral termination of the North-directed Alpine orogeny and onset of Westward escape in the Western Alpine arc: structural and sedimentary evidence from the external zone. Tectonics 30 (5). http://dx.doi.org/10.1029/2010TC002836.
Epard, J.L., Groshong Jr., R.H., 1993. Excess area and depth to detachment. AAPG Bull. 77 (8), 1291–1302.
Escher, A., Masson, H., Steck, A., 1993. Nappe geometry in the western Swiss Alps. J. Struct. Geol. 15 (3), 501–509. http://dx.doi.org/10.1016/0191-8141(93)90144-Y.
Etchecopar, A., Malavieille, J., 1987. Computer models of pressure shadows: a method for strain measurement and shear-sense determination. J. Struct. Geol. 9 (5), 667–677. http://dx.doi.org/10.1016/0191-8141(87)90151-9.
Ford, M., 1996. Kinematics and geometry of early Alpine, basement-involved folds, SW Pelvoux Massif, SE France. Eclogae Geol. Helv. 89 (1), 269–296.
Gratier, J.P., Vialon, P., 1980. Deformation pattern in a heterogeneous material: folded and cleaved sedimentary cover immediately overlying a crystalline basement (Oisans, French Alps). Tectonophysics 65 (1), 151–179. http://dx.doi.org/10.1016/0040-1951(80)90228-0.
Gratier, J.P., Lejeune, B., Vergne, J.L., 1973. Etude des d馭ormations de la couverture et des bordures s藏imentaires des massifs cristallins externes de Belledonne, des Grandes Rousses et du Pelvoux. Thesis 3e cycle Univ., Grenoble.
Groshong Jr., R.H., Epard, J.L., 1994. The role of strain in area-constant detachment folding. J. Struct. Geol. 16 (5), 613–618. http://dx.doi.org/10.1016/0191-8141(94)90113-9.
Guellec, S., Lajat, D., Mascle, A., Roure, F., Tardy, M., 1990. Deep seismic profiling and petroleum potential in the western alps: constraints with ECORS data, balanced cross-sections and hydrocarbon modeling. The Potential of Deep Seismic Profiling for Hydrocarbon Exploration. Edition Technip, Paris, pp. 425–437.
Henry, C., Burkhard, M., Goffe, B., 1996. Evolution of synmetamorphic veins and their wallrocks through a Western Alps transect: no evidence for large-scale fluid flow. Stable isotope, major-and trace-element systematics. Chem. Geol. 127 (1), 81–109. http://dx.doi.org/10.1016/0009-2541(95)00106-9.
Hoschek, G., 1980. Phase relations of a simplified marly rock system with application to the Western Hohe Tauern (Austria). Contribut. Minera. Petrol. 73 (1), 53–68. http://dx.doi.org/10.1007/BF00376260.
Lacombe, O., Mouthereau, F., 2002. Basement-involved shortening and deep detachment tectonics in forelands of orogens: Insights from recent collision belts (Taiwan, Western Alps, Pyrenees). Tectonics 21 (4), 1030. http://dx.doi.org/10.1029/2001TC901018.
Leloup, P.H., Arnaud, N., Sobel, E.R., Lacassin, R., 2005. Alpine thermal and structural evolution of the highest external crystalline massif: the Mont Blanc. Tectonics 24 (4). http://dx.doi.org/10.1029/2004TC001676.
Lemoine, M., Tricart, P., 1986. Les Schistes Lustrés piémontais des Alpes Occidentales: Approche stratigraphique, structurale et sédimentologique. Eclogae Geol. Helv. 79 (2), 271–294.
Lemoine, M., Gidon, M., Barféty, J.C., 1981. Les massifs cristallins externes des Alpes occidentales: d'anciens blocs basculés nés au Lias lors du rifting téthysien. C.R. Acad. Sci. Paris 292, 917–920.
Lemoine, M., Bas, T., Arnaud-Vanneau, A., Arnaud, H., Dumont, T., Gidon, M., Bourbon, M., De Graciansky, P.-C., Rudkiewicz, J.-L., Megard-Galli, J., Tricart, P., 1986. The continental magin of the Mesozoic Tethys in the Western Alps. Mar. Petrol. Geol. 3 (3), 179–199. http://dx.doi.org/10.1016/0264-8172(86)90044-9.
Lemoine, M., Dardeau, G., Delpech, P.Y., Dumont, T., De Graciansky, P.C., Graham, R., Jolivet, L., Roberts, D., Tricart, P., 1989. Extension synrift et failles transformantes jurassiques dans les Alpes occidentales. C.R. Acad. Sci. Sér. II Méc. Phys. Chim. Sci. Univ. Sci. Terre 309 (17), 1711–1716.
Letouzey, J., Werner, P., Marty, A., 1990. Fault reactivation and structural inversion. Backarc and intraplate compressive deformations. Example of the Eastern Sunda shelf (Indonesia). Tectonophysics 183 (1), 341–362. http://dx.doi.org/10.1016/0040-1951(90)90425-8.
Mennessier, G., Carme, F., Bellière, J., Dhellemes, R., Antoine, P., Dabrowski, H., Meloux, J., Bordet, C., 1977. Carte géologique de la France (1/50.000), feuille de Saint-Gervais-les-Bains. Bureau de Recherche géologique et minière, Orléans.
Moretti, I., Callot, J.P., 2012. Area, length and thickness conservation: Dogma or reality? J. Struct. Geol. 41, 64–75 http://dx.doi.org/10.1016/j.jsg.2012.02.014.
Mouthereau, F., Lacombe, O., 2006. Inversion of the Paleogene Chinese continental margin and thick-skinned deformation in the Western Foreland of Taiwan. J. Struct. Geol. 28 (11), 1977–1993. http://dx.doi.org/10.1016/j.jsg.2006.08.007.
Mouthereau, F., Watts, A.B., Burov, E., 2003. Structure of orogenic belts controlled by lithosphere age. Nature Geosci. 6 (9), 785–789. http://dx.doi.org/10.1038/ngeo1902.
Mugnier, J.L., Guellec, S., Menard, G., Roure, F., Tardy, M., Vialon, P., 1990. A crustal scale balanced cross-section through the external Alps deduced from the ECORS profile. Mém. Soc. Géol. Fr. 156, 203–216.
Oliver, N.H.S., 1996. Review and classification of structural controls on fluid flow during regional metamorphism. J. Metamorph. Geol. 14, 477–492. http://dx.doi.org/10.1046/j.1525-1314.1996.00347.x.
Oliver, N.H., Bons, P.D., 2001. Mechanisms of fluid flow and fluid–rock interaction in fossil metamorphic hydrothermal systems inferred from vein–wallrock patterns, geometry and microstructure. Geofluids 1 (2), 137–162. http://dx.doi.org/10.1046/j.1468-8123.2001.00013.x.
Panien, M., Schreurs, G., Pfiffner, A., 2005. Sandbox experiments on basin inversion: testing the influence of basin orientation and basin fill. J. Struct. Geol. 27 (3), 433–445. http://dx.doi.org/10.1016/j.jsg.2004.11.001.
Pfiffner, O.A., 1981. Fold-and-thrust tectonics in the Helvetic Nappes (E Switzerland). Geol. Soc. Lond. Spec. Publ. 9 (1), 319–327. http://dx.doi.org/10.1144/GSL.SP.1981.009.01.28.
Philippe, Y., Deville, E., Mascle, A., 1998. Thin-skinned inversion tectonics at oblique basin margins: example of the Western Vercors and Chartreuse Subalpine massifs (SE France). Geol. Soc. Lond. Spec. Publ. 134 (1), 239–262. http://dx.doi.org/10.1144/GSL.SP.1998.134.01.11.
Poty, B.P., Stalder, H.A., Weisbrod, A.M., 1974. Fluid inclusions studies in quartz from fissures of Western and Central Alps. Schweiz. Mineral. Petrogr. Mittl. 54, 717–752.
Ramsay, J.G., 1981. Tectonics of the Helvetic nappes. Geol. Soc. Lond. Spec. Publ. 9 (1), 293–309. http://dx.doi.org/10.1144/GSL.SP.1981.009.01.26.
Ramsay, J.G., Huber, M.I., 1989. The Techniques of Modern Structural Geology, vol. 2. Folds and Fractures Academic Press, London.
Ramsay, J.G., Casey, M., Kligfield, R., 1983. Role of shear in development of the helvetic fold-thrust belt of Switzerland. Geology 11 (8), 439–442. http://dx.doi.org/10.1130/0091-7613(1983)11<439:ROSIDO>2.0.CO;2.
Rolland, Y., Rossi, M., Cox, S.F., Corsini, M., Mancktelow, N., Pennacchioni, G., Fornari, M., Boullier, A.M., 2008. $^{40}Ar/^{39}Ar$ dating of synkinematic white mica: insights from fluid-rock reaction in low-grade shear zones (Mont Blanc Massif) and constraints on timing of deformation in the NW external Alps. Geol. Soc. Lond. Spec. Publ. 299 (1), 293–315. http://dx.doi.org/10.1144/SP299.18.
Roure, F., Colletta, B., 1996. Cenozoic inversion structures in the foreland of the Pyrenees and Alps. Mém. Mus. Natl. Nat. 170, 173–209.
Sanchez, G., Rolland, Y., Schneider, J., Corsini, M., Oliot, E., Goncalves, P., Verati, C., Lardeaux, J.-M., Marquer, D., 2011. Dating low-temperature deformation by $^{40}Ar/^{39}Ar$ on white mica, insights from the Argentera-Mercantour Massif (SW Alps). Lithos 125 (1), 521–536. http://dx.doi.org/10.1016/j.lithos.2011.03.009.
Scisciani, V., Tavarnelli, E., Calamita, F., Paltrinieri, W., 2002. Pre-thrusting normal faults within syn-orogenic basins of the outer Central Apennines, Italy: implications for Apennine tectonics. Bol. Soc. Geol. Ital. 121 (1), 295–304. http://dx.doi.org/10.1016/S0191-8141(01)00164-X.
Simon-Labric, T., Rolland, Y., Dumont, T., Heymes, T., Authemayou, C., Corsini, M., Fornari, M., 2009. 40Ar/39Ar dating of Penninic Front tectonic displacement (W Alps) during the lower oligocene (31–34 Ma). Terra Nova 21 (2), 127–136. http://dx.doi.org/10.1111/j.1365-3121.2009.00865.x.
Tavarnelli, E., 1999. Normal faults in thrust sheets: pre-orogenic extension, post-orogenic extension, or both? J. Struct. Geol. 21 (8), 1011–1018 http://dx.doi.org/10.1016/S0191-8141(99)00034-6.
Tricart, P., Lemoine, M., 1986. From faulted blocks to megamullions and mega-boudins: Tethyan heritage in the structure of the Western Alps. Tectonics 5 (1), 95–118.
Van Der Beek, P.A., Valla, P.G., Herman, F., Braun, J., Persano, C., Dobson, K.J., Labrin, E., 2010. Inversion of thermochronological age–elevation profiles to extract independent estimates of denudation and relief history—II: application to the French Western Alps. Earth Planet. Sci. Lett. 296 (1), 9–22. http://dx.doi.org/10.1016/j.epsl.2010.04.032.
Watts, A.B., Lamb, S.H., Fairhead, J.D., Dewey, J.F., 1995. Lithospheric flexure and bending of the Central Andes. Earth Planet. Sci. Lett. 134 (1), 9–21. http://dx.doi.org/10.1016/0012-821X(95)00095-T.
Yakovlev, F.L., 2012. Methods for detecting formation mechanisms and determining a final strain value for different scales of folded structures. C.R. Acad. Geosci. 344 (3), 125–137. http://dx.doi.org/10.1016/j.crte.2012.02.005.